VOLUMINA JURASSICA, 2025, XXIII: 43–64
DOI: 10.7306/VJ.23.2

Astrochronology of the Sinemurian Stage from the Llanbedr (Mochras Farm) core, NW Wales: Implications for the Early Jurassic timescale

Alexander J.L. HUDSON[1], Stephen P. HESSELBO[1, 2]*, Linda A. HINNOV[3], Kate LITTLER[1, 2], Kevin N. PAGE[1, 4], James B. RIDING[5], Micha RUHL[6], Clemens V. ULLMANN[1, 2]

Key words: Jurassic, Sinemurian, astrochronology, calcium content.

Abstract. Early Jurassic palaeoenvironments were perturbed during episodes of major global climate and biogeochemical change at the Triassic–Jurassic boundary and Early Toarcian Oceanic Anoxic Event (T-OAE). Other poorly understood palaeoclimate fluctuations and carbon-cycle perturbations occurred between these episodes, including the mid-Sinemurian Liasidium Event and the Sinemurian–Pliensbachian Boundary Event. Understanding of the causes and significance of these phenomena is limited by uncertainties in the geological timescale, particularly for the Sinemurian Stage. In this paper we present new multiproxy geochemical data through the Sinemurian and earliest Pliensbachian stages from the Llanbedr (Mochras Farm) borehole (NW Wales). The Mochras record is apparently stratigraphically complete except in the Upper Sinemurian which is affected by a normal fault that removes the lower part of the Oxynotum Zone. A floating astrochronology is developed for the Sinemurian Stage based on identification of the 405-kyr orbital eccentricity "metronome" in weight percent calcium and stable organic carbon isotopes ($\delta^{13}C_{org}$) from Mochras, together with data from the Robin Hood's Bay base-Pliensbachian GSSP section in Yorkshire, UK. The results indicate a minimum duration for the Sinemurian Stage of 7.3 Myr (7.1 Myr from Mochras and an additional 0.2 Myr from Robin Hood's Bay for the lower Oxynotum Zone). This interpretation of a long Sinemurian requires a short duration (~2 Myr) for the Hettangian stage.

INTRODUCTION

BACKGROUND AND AIMS

The Early Jurassic (201.4–174.1 Ma) biogeochemical systems were perturbed at several points in time by globally significant changes to the climate. The greatest of these occurred at the Triassic–Jurassic boundary at ~201.4 Ma, and in the Early Toarcian at ~183 Ma (*e.g.*, Korte *et al*., 2019; Schoepfer *et al*., 2022; Bos *et al*., 2024; Gambacorta *et al*., 2024). These events are associated with mass extinction (*e.g.*, Raup, Sepkoski, 1982; Little, Benton, 1995; Pálfy

[1] Camborne School of Mines, Department of Earth and Environmental Sciences, University of Exeter, Penryn Campus, Cornwall TR13 0DB, UK; ajlhudson@hotmail.co.uk, s.p.hesselbo@exeter.ac.uk, k.littler@exeter.ac.uk, c.ullmann@exeter.ac.uk.
[2] Environment and Sustainability Institute, University of Exeter, Penryn Campus, Cornwall TR13 0DB, UK.
[3] Department of Atmospheric, Oceanic and Earth Sciences, George Mason University, Fairfax, VA 22030, USA; lhinnov@gmu.edu.
[4] Geodiversity & Heritage, Thornedges, Sandford, Crediton, Devon, EX174BR; kevinnpage@gmail.com.
[5] British Geological Survey, Keyworth, Nottingham NG12 5GG, UK; jbri@bgs.ac.uk.
[6] Department of Geology, Trinity College Dublin, The University of Dublin, College Green, Dublin, Ireland; ruhlm@tcd.ie.
* Corresponding author.

et al., 2000; Wignall, 2001; Cecca, Macchioni, 2004; Caruthers *et al*., 2013; Wignall, Atkinson, 2020; Lindström, 2021), oceanic and marine-shelf anoxia (Jenkyns, 1988, 2010; van de Schootbrugge *et al*., 2013), likely extreme temperature fluctuations including greenhouse warming (Korte *et al*., 2009; Pieńkowski *et al*., 2016; Ruebsam *et al*., 2020; Ullmann *et al*., 2020) and some of the largest perturbations to the global carbon cycle in the Mesozoic (Hesselbo *et al*., 2000, 2002, 2007; Pálfy *et al*., 2001; Jenkyns *et al*., 2002; Kemp *et al*., 2005; Pieńkowski *et al*., 2016; Ruhl *et al*., 2020; Storm *et al*., 2020). Both the Triassic–Jurassic mass extinction and the Toarcian Oceanic Anoxic Event have been convincingly linked to climate forcing by igneous processes associated with large igneous provinces that occurred at the same time (*e.g.*, Pálfy, Smith, 2000; Cohen, Coe, 2002; Suan *et al.*, 2010; Burgess *et al*., 2015; Percival *et al*., 2015, 2016; Davies *et al*., 2017; Heimdal *et al*., 2020; Ruhl *et al*., 2022; Bos *et al*., 2024; Fendley *et al*., 2024).

The intervening ~18 Myr of the Early Jurassic (the Hettangian–Pliensbachian stages) has yielded evidence for more modest but potentially regular oscillations to the exogenic carbon reservoir, as expressed by carbon-isotope values of marine and terrestrial organic matter and carbonate (Ruhl *et al*., 2010; Korte, Hesselbo, 2011; Jenkyns, Weedon, 2013; Riding *et al*., 2013; Duarte *et al*., 2014; Franceschi *et al*., 2014; Porter *et al*., 2014; Xu *et al*., 2017; Hesselbo *et al*., 2020a, b; Storm *et al*., 2020; Pieńkowski *et al*., 2020; Ullmann *et al*., 2021). Short duration (<1 Myr) negative carbon-isotope excursions (CIE's) in the Sinemurian have been associated with episodes of supposed climate warming (Jenkyns *et al.*, 2002; Korte, Hesselbo, 2011; Jenkyns, Weedon, 2013; Riding *et al.*, 2013; Hesselbo *et al.*, 2020b), whilst the late Pliensbachian positive carbon-isotope excursion is suggested to be associated with at least regional cooling (Korte, Hesselbo, 2011; Korte *et al*., 2015; Ruebsam *et al*., 2019; Hollaar *et al*., 2023). On longer, multi-million year, timescales the carbon-isotope ratios of marine dissolved inorganic carbon and sea-water temperature are not so clearly linked (Korte *et al*., 2015; Hesselbo *et al*., 2020a).

Understanding climatic events in the Early Jurassic requires a precise global timescale. For the Jurassic, radioisotopic ages from ash beds in South America (Schaltegger *et al*., 2008; Schoene *et al*., 2010; Wotzlaw *et al*., 2014; Al-Suwaidi *et al*., 2022) are tied to mostly European marine sedimentary records (Ruhl *et al*., 2010, 2016, 2022; Storm *et al*., 2020) through chemostratigraphic and biostratigraphic correlation (see *e.g.*, summary in Hesselbo *et al*., 2020c). Astronomical timescales are developed for the Hettangian (Ruhl *et al.*, 2010; Weedon *et al.*, 2019), the Pliensbachian (Ruhl *et al.*, 2016; Pieńkowski *et al*., 2021) and the Toarcian (Kemp *et al.*, 2005; Suan *et al*., 2008; Boulila *et al*., 2014; Pieńkowski *et al*., 2024) stages of the Jurassic based on the expression of Milankovitch cycles of precession, obliquity, and eccentricity in these marine sedimentary successions. However, the Sinemurian Stage has proven more difficult to calibrate, due to a lack of suitable long and apparently complete successions with good ammonite biochronostratigraphic control, and for GTS2020 (Hesselbo *et al.*, 2020c) the length of the Sinemurian was estimated only by cyclostratigraphic calibration of the adjacent stages (6.6 Myr long).

Otherwise excellent chemostratigraphic records have lacked one or more important attribute sufficient to analyse the full spectrum of Milankovitch cycles for the entire stage, such as radiometric or biostratigraphic calibration (Ikeda, Tada, 2014), length and completeness (Jenkyns, Weedon, 2013; Schöllhorn *et al*., 2020) or sample resolution (Storm *et al*., 2020). Recent work on a new borehole, the Prees 2 borehole in the Cheshire Basin, Shropshire, UK, has shed new light on the Rhaetian to lower Pliensbachian, but also lacks a complete upper Sinemurian section (Hesselbo *et al*., 2023; Leu *et al*., 2024).

Construction of an astrochronology for the Sinemurian is further complicated by the uncertainty surrounding the durations of neighbouring stages. The age of the Hettangian–Sinemurian boundary is constrained through anchored astrochronologies from the lacustrine record in the Newark and Hartford basins, USA, and shallow marine coastal record of Somerset, UK, yielding a consistent 1.9 Myr duration for the Hettangian (Ruhl *et al*., 2010; Kent *et al*., 2017; Huang, 2018) anchored to the radiometric age of the T-J boundary (201.4 Ma; Schaltegger *et al*., 2008; Schoene *et al*., 2010; Wotzlaw *et al*., 2014). However, more recently a study of multiple basins in the UK (including re-interpretation of the same Somerset coastal section studied previously) yielded a far longer ≥4.1 Myr duration for the Hettangian stage (Weedon *et al*., 2018, 2019). This latter study postulated multiple hiatuses within different sections to argue for missing time in the records from each basin and thus, through construction of a composite, yielded a much longer total duration for the stage. The varying durations estimated for the bounding stages of the Sinemurian thus give a broad and uncertain time-window for the Sinemurian stage ranging from ~7.0 to 4.2 Myr. Indeed, the Sinemurian stage now represents a keystone interval for a complete integrated timescale for the Early Jurassic.

The onshore basins of the United Kingdom preserve relatively continuous marine sedimentary records from the Early Jurassic and have been foundational for development of the ammonite chronostratigraphic scheme that underpins the Early Jurassic timescale (Cope *et al*., 1980; Cox, 1990; Page, 2003, 2010a, 2017). Excellent coastal exposures have been used to define Global Stratotype Sections and Points (GSSPs) for the base-Sinemurian at East Quantoxhead, Somerset (Bloos, Page, 2002), and the base-Pliensbachian at Robin Hoods Bay, Yorkshire (Meister *et al*., 2006). Moreover, boreholes drilled in the 1960's and 1970's have yielded a series of cores and core samples that complement the coastal exposures with generally more continuous records of the Early Jurassic, and which are available for study at the British Geological Survey National Core Repository at Keyworth, Nottingham, UK.

Here, we present new data from previously unexploited borehole material from onshore UK and integrate with results from the coastal exposures that host the two GSSP's (Fig. 1). The new analyses are from the Llanbedr (Mochras Farm) Borehole – also known as Mochras – in the Cardigan Bay Basin, the succession from which is stratigraphically expanded and also stratigraphically complete at the ammonite chronozone level (Wood, Woodland, 1968; Woodland

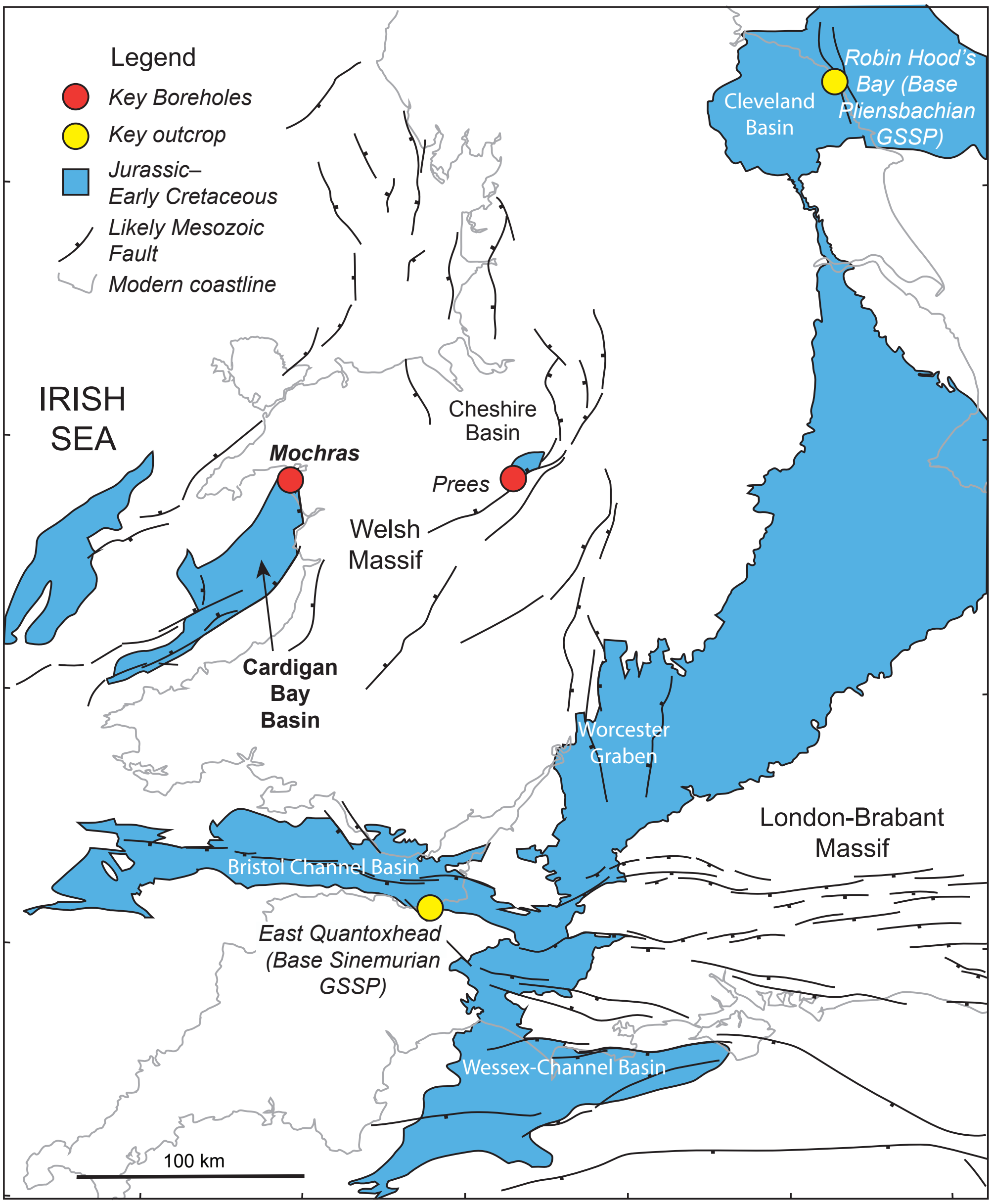

Fig. 1. Key localities discussed in the text

The Llanbedr (Mochras Farm) borehole is located on the eastern preserved edge of the Cardigan Bay Basin. Figure based on BGS 1:1,500,000 series tectonic map of Britain, Ireland and adjacent areas, Sheet 1 (Pharaoh, 1996) and is modified from Hesselbo *et al.* (2023)

1971; Dobson, Whittington 1987; Hesselbo *et al*., 2013, 2023; Copestake, Johnson 2014; Pieńkowski *et al*., 2024). We use here a multi-proxy approach to understand the mechanisms that imprint Milankovitch cyclicity in this marine record and compare the Mochras record with that from the Robin Hood's Bay coastal exposures (Hudson *et al*., 2025), to construct an astronomically calibrated floating timescale for the whole Sinemurian. The significance of the new timescale is then discussed with reference to estimated durations of the underlying Hettangian stage.

GEOLOGICAL SETTING

During the Jurassic Period, the UK area comprised a series of sedimentary basins that developed in response to widespread lithospheric extension across NW Europe from the Permian to Cretaceous periods (*e.g.*, Ziegler, 1990; Cope *et al*., 1992; Bjerrum *et al*., 2001; Powell, 2010). The latest Triassic is marked by a widespread marine transgression across northern Europe (Arkell, 1933, 1956; Hallam, 2001; Pieńkowski, 2004; Pieńkowski *et al*., 2008). In the Jurassic, the UK area was part of a generally shallow marine epicontinental shelf, populated with a series of small islands separated by subsiding basins controlled by E–W, N–S or NE–SW fault systems (*e.g.*, Hesselbo, 2012). The Mochras borehole (Cardigan Bay Basin, Wales), and the Robin Hoods Bay section (Cleveland Basin, Yorkshire, England) record marine successions from two of these distinct subsiding sedimentary basins (Fig. 1; Woodland, 1971; Powell, 2010). The records from almost all the onshore UK sedimentary basins comprise relatively shallow-marine storm-influenced facies (Sellwood, 1970; Hesselbo, Jenkyns, 1995; van Buchem, Knox, 1998; Powell, 2010; Hesselbo *et al*., 2020b) whilst, exceptionally, the Lower Jurassic of the Cardigan Bay Basin is interpreted, on the basis of trace fossils and facies sequences, as deposited in relatively deep water, below storm wave base and with sediment transport by contour currents (Pieńkowski *et al*., 2021, 2024).

The Mochras borehole, located in the footwall of the prominent Mochras Fault, at the eastern end of the Cardigan Bay Basin, recorded an unexpectedly thick ~1300 m succession of Hettangian–Toarcian argillaceous strata, the thickest onshore UK Lower Jurassic succession known (Wood, Woodland, 1968; Tappin *et al.*, 1994). The borehole was drilled in 1969 by Aberystwyth University and the British Geological Survey and terminated at 1938.4 mbs in the Upper Triassic.

The Sinemurian Stage is well defined by ammonite fossils, with ~500 m of Sinemurian strata preserved at Mochras. Lower Jurassic strata are referred to the Lias Group across the whole of the UK area, and in southern England and Wales the lower Lias Group is subdivided into the Hettangian–Sinemurian Blue Lias Formation (Cox *et al*., 1999) comprising limestone/mudstone interbeds, and a Sinemurian–Pliensbachian Charmouth Mudstone Formation composed predominantly of mudstone. Both formations have abundant marine macrofossils, including bivalves, brachiopods, crinoids, and ammonites; in Mochras the Lias Group has not been formally subdivided into formations, but the broad pattern of reduction up-section in carbonate content evident elsewhere is present (*e.g.*, Ullmann *et al.*, 2021).

The Mochras borehole was fully cored with nearly 100% recovery, but much of the core was broken up shortly after it had been retrieved. Some of this material was used for macrofossil biostratigraphy, with much of the remainder archived at the UK National Core Repository or distributed to third parties (a set of Mochras subsamples is presently maintained at the Rutgers University Core Repository New Jersey, USA). The rock samples worked on for this study utilise the 'registered specimens', 'reserve samples' and 'archive core slabs' at the National Core Repository, Keyworth. Registered specimen refers to samples that were collected usually based on features of palaeontological interest, and commonly embedded in core whole rounds, with the depths of each specimen precisely recorded. 'Reserve sample' refers to bags of gravel-sized fragments, collected from a stratigraphic thickness of on average 5 feet in the case of Mochras; these samples have no clear bedding context, contain few fossils, and stratigraphic precision is limited by the collection interval. Multiple bags were in some cases collected from the same intervals. Archive core slabs are generally ½ rounds for the Sinemurian where they exist.

PREVIOUS RECORDS OF CYCLICITY

The Lower Jurassic has previously yielded evidence for Milankovitch cyclicity in the Lias Group from the Wessex and Bristol Channel basins (Weedon, 1986; Smith, 1989; Waterhouse, 1999; Weedon, Jenkyns 1999; Weedon *et al*., 1999, 2018, 2019; Bonis *et al*., 2010; Clémence *et al*., 2010; Ruhl *et al*., 2010; Hüsing *et al*., 2014; Xu *et al*., 2017; Huang, 2018), the Cheshire Basin (Hesselbo *et al*., 2023; Leu *et al*., 2024), the Cleveland Basin (van Buchem, McCave, 1989; van Buchem *et al*., 1992, 1994; Hesselbo, Jenkyns, 1995), and the Cardigan Bay Basin (Ruhl *et al*., 2016; Storm *et al*., 2020; Pieńkowski *et al*., 2021, 2024; Hollaar *et al*., 2021, 2023, 2024).

In the Bristol Channel Basin, particularly along the well-studied coastal exposures where the base-Sinemurian GSSP is situated (Fig. 1), the Blue Lias Formation shows Milankovitch frequency cyclicity in both carbonate content (Weedon *et al*., 2019) and in organic matter content and organic carbon-isotope values (Ruhl *et al*., 2010; Xu *et al*., 2017). However, in detail, there are significant differences in interpretation. For example, Ruhl *et al.* (2010) identified cyclicity at a 4 to 6 m scale which they assigned to short eccentricity based on the observed lithological bundling. In contrast, Weedon *et al.* (2019) argue that particularly in the earliest Jurassic Tilmanni and Planorbis ammonite chronozones, sedimentary cyclicity at ~70–80 cm is the 100-kyr eccentricity signal, with a substantial increase in sedimentation rate after deposition of these earliest Jurassic strata.

In the Cardigan Bay Basin, Mochras borehole, metre-scale astronomical precession-related couplets of carbonate-rich silty beds and carbonate-poor clay-rich beds occur strongly through the Pliensbachian and Toarcian stages, and these show a bundling and lithological variation that is consistent with a Milankovitch imprint including obliquity, and short and long eccentricity cycles (Ruhl *et al.*, 2016; Hollaar *et al*., 2023), as well as potentially long-duration so-called grand eccentricity cycles at a periodicity of 2.4 Myr (Pieńkowski *et al.*, 2021, 2024).

Spectral analysis of low-resolution carbon-isotope geochemistry from Mochras core samples suggests a stable 405 kyr metronome also running throughout the Early Jurassic (Storm *et al.*, 2020), including through the relatively understudied Sinemurian part of the core. Those few intact core slabs that are preserved for the Mochras Hettangian and Sinemurian also show strong evidence of metre-scale lithological cyclicity that can hypothetically be related to precession (Hesselbo *et al.*, 2013; Storm *et al.*, 2020).

It is clear from these detailed outcrop studies, and previous borehole analysis, that the Sinemurian of the Mochras borehole has the potential to faithfully record Milankovitch frequency cyclicity.

METHODS

SAMPLES AND DATA SOURCES

A total of 1150 registered specimens and 403 archive core slabs were used to generate ‘Device B’ portable X-Ray Fluorescence (p-XRF) data (see next Section below for further explanation), and the Ca values are published in Ullmann *et al.* (2021). Another set of 193 measurements were made from registered specimen offcuts which have not been previously published and pertain to ‘Device A’. All of these samples and data have precise depth information and a median sample spacing of 25 cm. These data are supplemented with measurements made from the reserve sample set, whose depths are imprecisely known (comprising a ~1.4 m stratigraphic range) but generally regularly spaced and ranging through the whole stage. Such data include 185 Rock Eval pyrolysis-based Ca content data (Storm *et al.*, 2020). The addition of this sample set closes some sample gaps and improves the median resolution to 23 cm. All data are included in Supplementary Data Files 1, 2 and 3.

PORTABLE X-RAY FLUORESCENCE (P-XRF)

Elemental data were obtained from samples of the matrix of solid rock cut from the selected registered specimens and core samples as inventoried above. The p-XRF analysis was conducted on flat-cut surfaces of rock, comparable to using full cut core as practised by Ruhl *et al*. (2016). Olympus Innov-X Delta Premium XRF Analyzers at the University of Exeter, Camborne School of Mines, were used set to ‘Geochem’ mode. Readings were collected for 50 s each for voltages of 40 and 10 kV, capturing the trace and major element concentrations from Mg to Pb. Reproducibility of the measurements was controlled through interspersed measurements of the standard NIST 2710a (every 10th sample); see Supplementary Data Files 2, 3. Sample heterogeneity was modelled through the analysis of representative samples many times in different parts of the same samples. Two instruments were used, devices A and B; results from each were cross calibrated by measurement of an overlapping sample set (n = 12, details provided in the Supplementary Data Files 4, 5). The p-XRF results can only be regarded as semi-quantitative, due to matrix and instrumental effects, with the accuracy of the signal constrained through repeat measurements of the standard. The p-XRF measurement positions were designed to avoid sample complications due to intersecting fossils (anomalously high Ca) or pyrite nodules (anomalously high Fe and S).

TIME SERIES METHODS

The analysis package Acycle (v2.1; Li *et al*., 2019) was used for the time series analysis. Core depth series data were pre-processed for time series analysis using a typical methodology involving three steps: 1) removal of outliers using the R boxplot algorithm to remove data points that fall outside of the 95% confidence interval of the median value; 2) linear interpolation to the median sample spacing in Acycle using the ‘interpolation’ function, and; 3) detrending in order to bring the data towards a long-term stationary mean in Acycle (‘Detrend’ function). Further parameterisation is described in the next Section.

Initial analysis was conducted in the core depth domain. Power spectra were computed using the multi-taper method (MTM) with AR1 classical red noise modelling for analysis of the geochemical depth series. The power spectra were examined for the typical ratio of spectral peaks that is expected from Milankovitch cyclicity and compared with the results of visual cycle analysis.

Sedimentation rate analysis was conducted on the weight percent Ca record using the Average Spectral Misfit (ASM) method (Meyers, Sageman, 2007) as implemented in Acycle (Li *et al.*, 2018). The data were tuned to a bandpass filter in the depth domain, that corresponded to the hypothesised 405 kyr long orbital eccentricity cycle in the data, as inferred from visual analysis of the Ca data. Subsequently, the power spectra of the time-converted data series were examined for the orbital eccentricity, obliquity and precession index as calculated for the Early Jurassic (Waltham, 2015). Uncertainty in the interpretation, while subjective, was estimated from the range of possible cycles identified from visual analysis versus the number of cycles in the bandpass filter that was used to time-convert the dataset. Further detail on the treatment of the data and generation of the age model are outlined below in the Section below.

RESULTS

GENERAL OBSERVATIONS AND PRINCIPAL DATASETS

The uppermost Sinemurian to Toarcian of the Mochras borehole, for which core slabs are still available, is characterised by primary cycles of alternating pale-medium grey argillaceous calcareous silty mudstone and darker grey, sometimes laminated micaceous silty mudstone (Ruhl *et al*., 2016; Hollaar *et al.*, 2021, 2023, 2024; Pieńkowski *et al*., 2021, 2024). Sporadic carbonate nodules are also present, and some thin argillaceous limestone beds may also represent conjoined nodules (Pieńkowski *et al*., 2021). These cyclic alterations are picked out through varying colour and hardness which are visual proxies for carbonate content. Based on ichnofacies and lithofacies sequences, the environment of deposition is interpreted as below storm wave base, with cyclicity governed by fluctuation in bottom (contour) current strength (Pieńkowski *et al*., 2021, 2024).

Similar characterisation of the sedimentary cycles for most of the Hettangian–Sinemurian interval is limited by the preservation of only a few intact core slabs; however, the likely ubiquitous presence of metre scale cycles can be assumed based on those slabs that are preserved (*e.g.*, Hesselbo *et al*., 2013), alongside the very strong expression of metre-scale precession in higher parts of the Mochras Lower Jurassic, where orbitally-tuned age models exist.

A high resolution ammonoid biochronology of the Sinemurian interval of the Mochras borehole was established though a search of nearly 6,500 registered borehole specimens housed in the British Geological Survey (BGS) collections. The affinities of the fauna correspond to the North-West European Province (Page, 2008) and hence the chronozonal scheme applied is that of Dean *et al*. (1961) and later reviewed by Page (2003). Ammonoid faunas were correlated against the latest scheme of 77 biohorizons applicable to the province (see Page, 2010a, b), although the limits of sampling a relatively small core diameter mean that the limits of subzones are quite uncertain.

A fault has been interpreted to cut the Sinemurian strata at 1372 mbs, associated with fractured rock, slickenlines, and calcite veining (Fig. 2; Woodland, 1971; Ullmann *et al*., 2021). The revised ammonite zonation in Hesselbo *et al*. (2023) shows that the base of the Oxynotum Zone coincides (within uncertainty) with the level of the fault; given that the lower subzone of the Oxynotum Zone (*i.e.* the Simpsoni Subzone) is unproven, it is likely that an extensional fault cuts out the lower Oxynotum Zone and, potentially, some smaller portion of the uppermost Obtusum Zone.

Portable XRF data for calcium show strong inverse linear relationships with Si, Al, Rb, Zr, K, Ti and Fe through the Sinemurian section at Mochras (Fig. 3). Calcium is primarily incorporated in calcite which, from petrographic studies, makes up the principal carbonate mineral in the Mochras borehole (Ullmann *et al*., 2021), and calcium carbonate content has a strong dilution effect on other elements. The elements Si and Zr are commonly associated with silt to fine sand grade quartz and zircon, respectively, while Al, K and Rb are commonly contained in aluminosilicates, giving an approximation of clay abundance (and grain size) in other comparable successions (*e.g.*, Hesselbo *et al*., 2020b; LaGrange *et al*., 2020; Thöle *et al*., 2020). Calcium shows no linear correlation to Si/Al, Zr/Rb or to redox sensitive elements Mo, and S (commonly associated with sulphides) suggesting that the carbonate dilution in the Sinemurian section is neither entirely diagenetic nor solely associated with the clastic grain size (Figs. 2, 3). It is likely that varying siliciclastic flux as well as diagenetic enrichment may have affected the carbonate content in the Mochras borehole lithologies. It is also possible that different processes control the patterns in Ca in individual (orbitally-paced) cycles, versus longer term trends at Mochras (the Mochras Pliensbachian precession cycles show a marked positive relationship between carbonate content and inferred grain size; Hollaar *et al*., 2023).

VISUAL INTERPRETATION OF CYCLICITY

Calcium values from XRF range between 0.83% and 45.8% with an average value of 16.4% (Fig. 2). The Bucklandi Zone shows high amplitude variations in Ca content that align well with descriptions of marl or limestone beds in

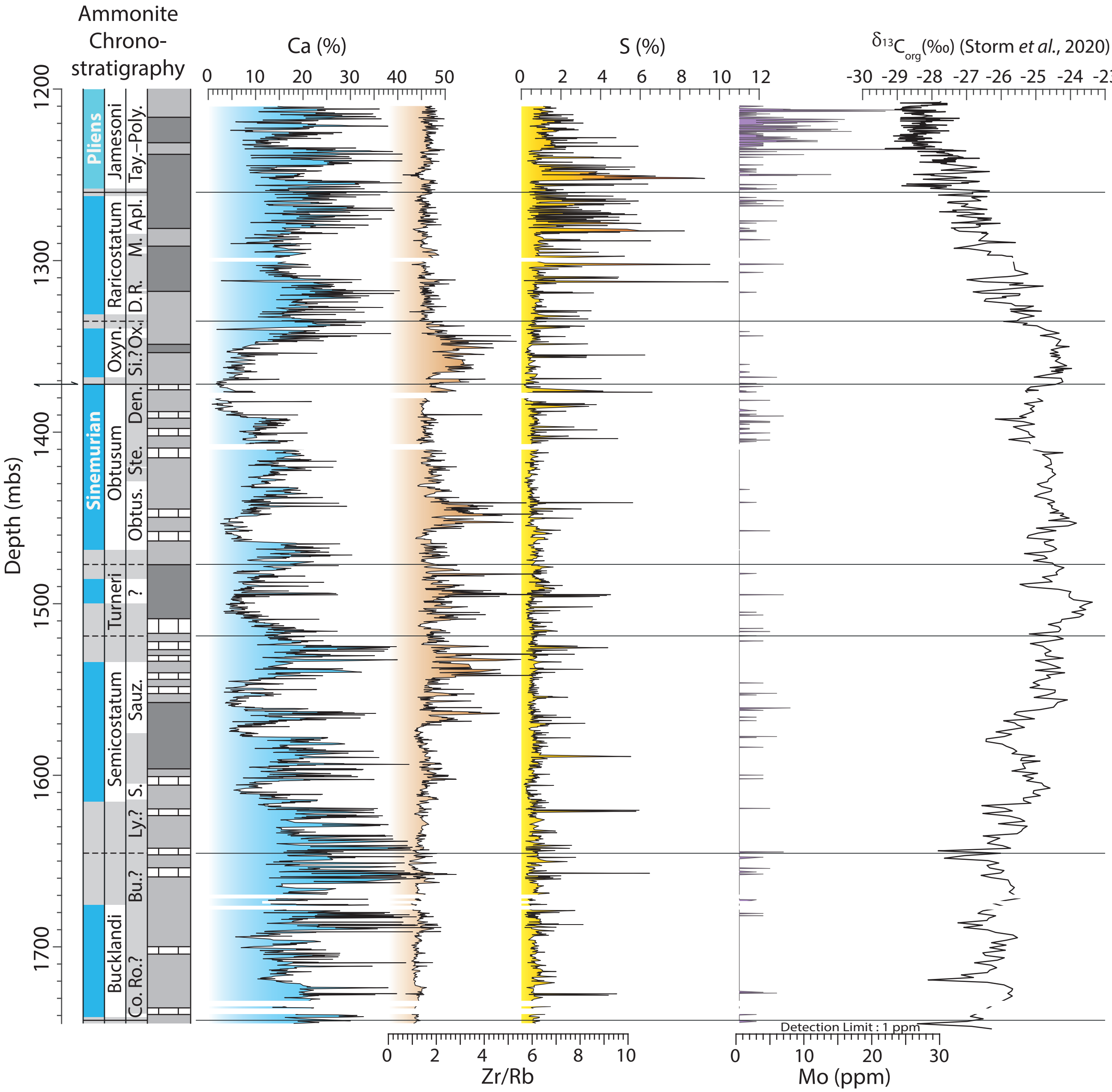

Fig. 2. Compilation of key datasets for Mochras

Ammonite chronostratigraphy from Woodland (1971), Page in Copestake and Johnson (2014), Hesselbo *et al.* (2023), and Page *et al.* (2025). Percentage Ca is based on p-XRF Ca content (this study, Ruhl *et al.*, 2016) and Rock Eval pyrolysis data (Storm *et al.*, 2020). Stable carbon isotope data from bulk organic matter are from Storm *et al.* (2020). Fault position at 1372 mbs from Woodland (1971). All other data are from the present study and based on p-XRF measurements. The Mo content is commonly below detection limit (1 ppm). The Zr/Rb ratio is used here as grain-size proxy and suggests slightly coarser-grained (i.e. silty) sediments in the late Semicostatum to early Obtusum zones, and the Oxynotum Zone. Higher Mo and S concentrations reflect likely development of dysoxic conditions on the seafloor. Anomalous wider sample spacing (>1.5 m) is indicated with line and shading gaps which is either due to original core loss or lack of registered specimens

the wellsite sedimentary log. Intervals of generally Ca-rich (up to 45%) and Ca-poor (down to ~1%) samples define large-scale, 30–24 m, oscillations through the section. Several extended intervals of very low calcium values (2–5%) occur primarily at ~1605 mbs (mid Semicostatum Zone), ~1580–1555 mbs (upper Semicostatum Zone), ~1500 mbs

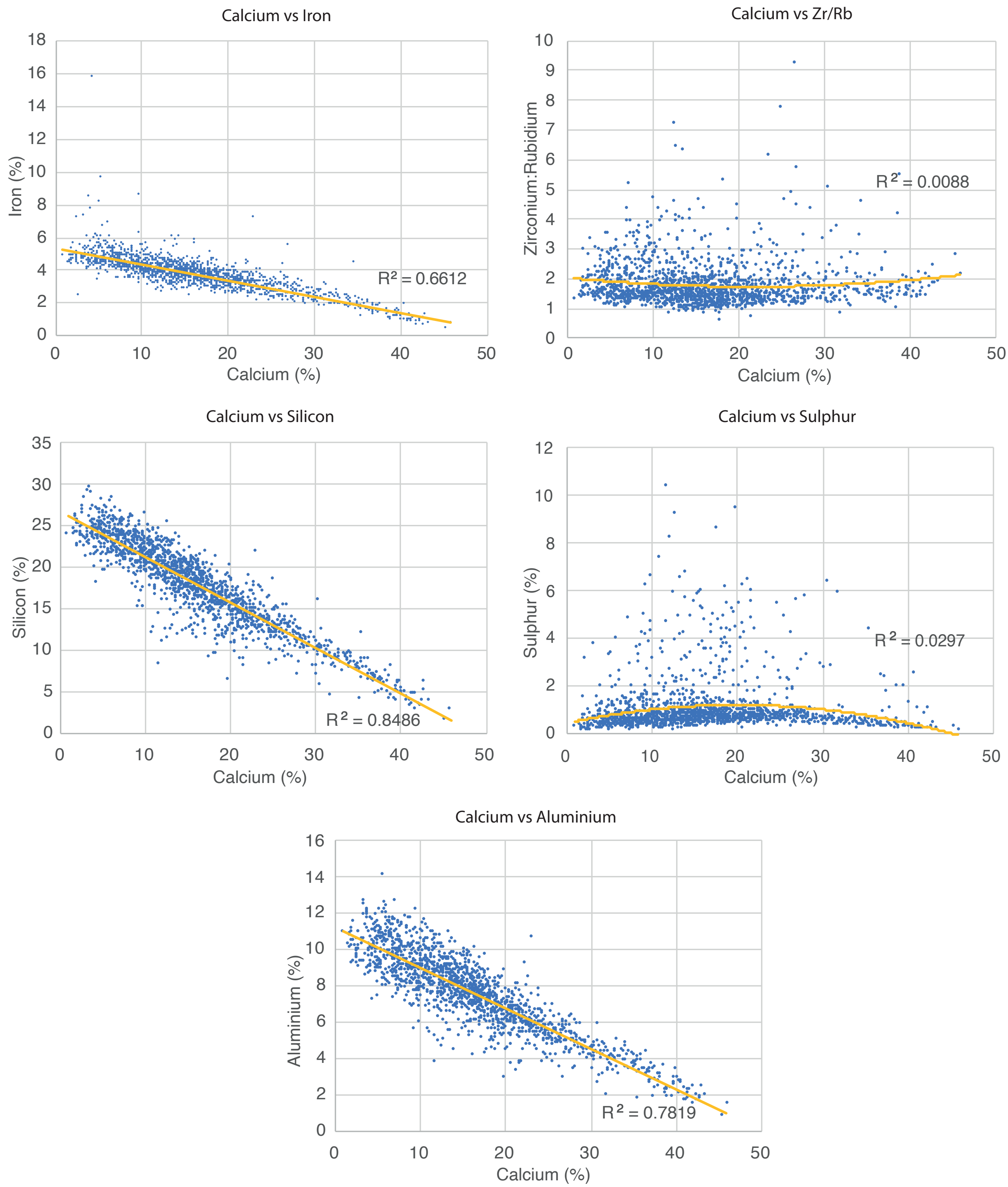

Fig. 3. Cross-plots of p-XRF elemental data from Mochras demonstrating a strong inverse linear correlation between calcium and elements with a primarily terrigenous source such as Fe, Al and Si

This relationship is indicative of a sedimentary dilution effect rather than diagenesis, illustrated by the poor correlation of Ca with other elements such as S (mid Turneri Zone), ~1460 mbs (base Obtusum Zone) and 1390–1370 mbs (Obtusum–Oxynotum zonal boundary).

For grain-size proxies the trends are identical between Si/Al and Zr/Rb (Supplementary Data Files 2, 3), and oscillations show similar scales, even if they are generally out of synchrony with trends seen in Ca%. Values of Zr/Rb are low at the base of the Sinemurian section, indicating fine grained sediment, gradually increasing throughout the Bucklandi and lower Semicostatum zones up to 1577 mbs, where there is an abrupt jump to much higher but oscillating values in the upper Semicostatum and Turneri zones, indicative of a coarser clastic component (Fig. 2). The Obtusum Zone is characterised by initially low values (i.e. finer grained), rising to a high point at ~1445 mbs, and followed upwards by a gradual decrease to a minimum at the Obtusum–Oxynotum boundary. The Oxynotum Zone has high values again, dropping abruptly to low values through the Raricostatum Zone, and the Jamesoni Zone of the Pliensbachian, indicating a return to finer siliciclastic grain size.

Redox sensitive elements are on average very low in content, in concordance with the relatively low TOC (~1%)

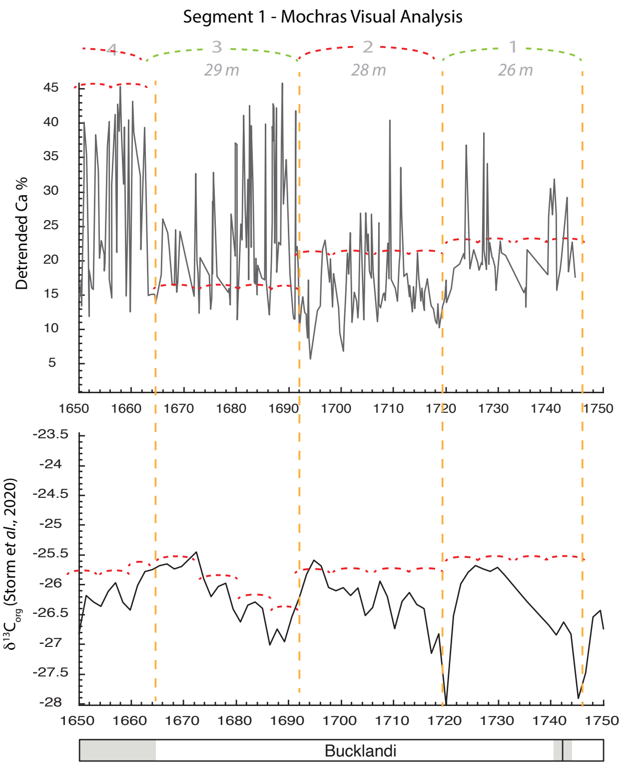

Fig. 4. Example of visual interpretation of nested cycles for the Bucklandi Zone

Large scale cycles (C1, ~30 m scale) contain ~4 nested smaller scale cycles (C2, ~4–6 m). For full detail of visual interpretation across the entire Sinemurian Stage, see Hudson (2021)

measured for the Sinemurian (Storm *et al*., 2020). Molybdenum (Mo) is mostly below detection limit, but rises locally to a maximum of 32 ppm at the top of the studied section. Detection occurs weakly between 1405 and 1365 mbs (Obtusum–Oxynotum zones) and strongly between 1286 and 1212 mbs (Raricostatum–Jamesoni zones, especially the latter). Sulphur (S), allied closely to sulphide in the form of pyrite, also rises significantly in the Raricostatum and Jamesoni zones.

The $\delta^{13}C_{org}$ time series (bulk organic matter) shows a long-term stratigraphic trend rising from the base of the Sinemurian to an Early Jurassic high of –23.4‰ in the Turneri Zone, and then a stepped decrease to the mid-Jamesoni Zone in the earliest Pliensbachian (Storm *et al*., 2020). Superimposed onto this trend are a series of 20–30 m scale 1–2‰ oscillations in $\delta^{13}C_{org}$. The lightest values occur on this beat as sharp negative spikes, *e.g.* at ~1720 mbs (Bucklandi Zone). Several more extended intervals of isotopically lighter organic carbon isotopes occur, notably at 1660–1640 mbs in the Bucklandi–Semicostatum zonal transition, and 1405–1375 mbs in the upper Obtusum Zone in the mid-Sinemurian. The sampling rate of the $\delta^{13}C_{org}$ data (~1.4 m average, compared to 0.23 m for Ca) may be responsible for aliasing the underlying variability, particularly in the Raricostatum and Jamesoni zones (see Hollaar *et al*., 2024 who show a higher resolution dataset).

TIME SERIES ANALYSIS

Apparently periodic oscillations in all the datasets are observed on the primary scale of ~20–30 m, a cyclicity here termed C1. These are superimposed on longer period variations at a length scale of around 100 m or greater. Within the C1 cycles are typically bundles of ~4 shorter cycles at ~6 m scale, termed here C2, as illustrated in Figure 4 (full detail set out in Hudson, 2021). Through the whole Sinemurian succession, 17–18 C1 cycles are observed ranging from 21 to 33 m in thickness with a median of 28 m (Fig. 5).

All data were linearly interpolated to the median sample spacing (Ca composite at 23 cm; $\delta^{13}C_{org}$ at 1.2 m), and detrended using a 114 m (Ca composite, $\delta^{13}C_{org}$) locally estimated scatterplot smoothing technique (rLOESS). The 114 m rLOESS method was chosen to remove the long trends identified in provisional analysis that were present at ~495 m (close to series length), 190 m and 116 m periods.

Application of the ASM test indicates that the sedimentation rate for the Sinemurian at Mochras was not constant (Fig. 6). Four sedimentation rates have a null hypothesis significance level of 1%, at 6.1, 7.2, 7.8–8.1 and 9.2 cm/kyr. These values are somewhat higher than those calculated for the subsequent Pliensbachian (4.5–5.1 cm/kyr; Pieńkowski

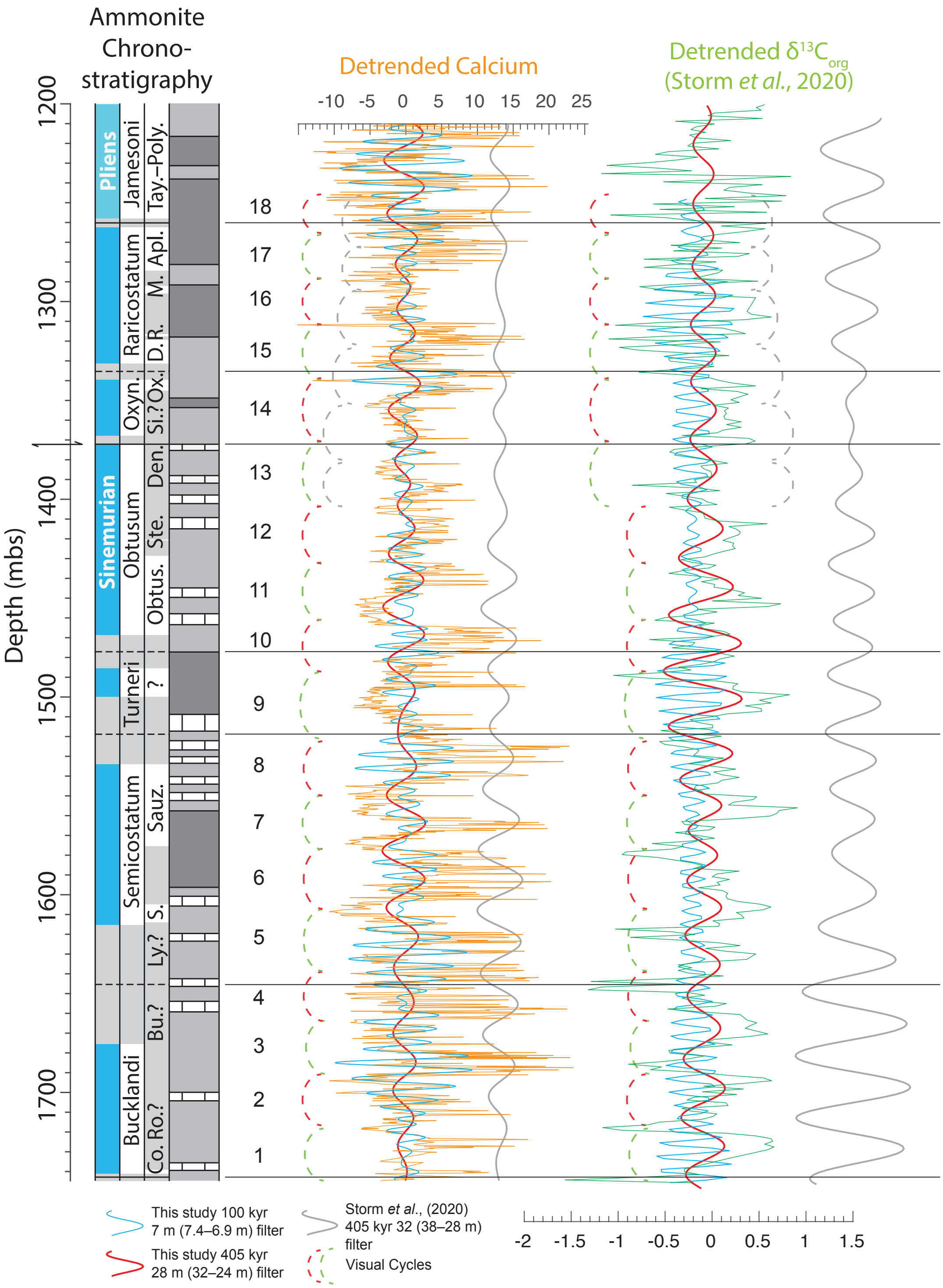

Fig. 5. Detrended Ca content data (orange line) and carbon isotopes (green line) for the whole Sinemurian at Mochras, together with cycles derived from visual analysis of these data (dashed red and green lines, labelled 1–18)

Also shown are the Gaussian bandpass filters as applied to these datasets for specific periods (28 ±4 m, which we infer to represent the 405 kyr cycle (red line), and 7.00 ±0.25 m which we infer to represent the 100 kyr cycle (blue line)), compared to those used for Storm *et al.* (2020; grey). Fault is shown at 1372 m at the base of the Oxynotum Zone

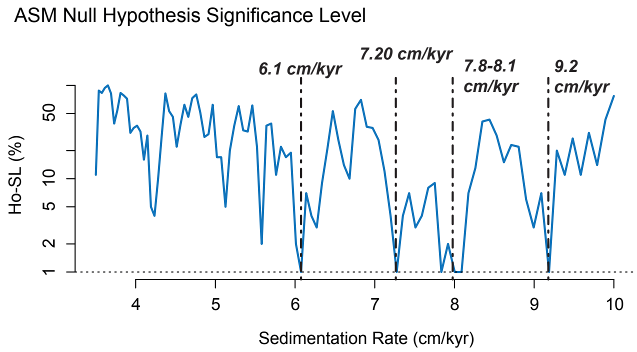

Fig. 6. Results of sedimentation rate analysis for the Mochras Sinemurian (Average Spectral Misfit (ASM) based on composite Ca depth series

Sedimentation rates are estimated to vary between 6.1 and 9.2 cm/kyr

et al., 2021) concordant with a long-term slowing of accumulation through the Early Jurassic at this site.

The MTM power spectra are shown in Figure 7. For all elemental proxies and methods, power is consistently concentrated at wavelengths of 31, 24, 7.6–6.7, 2.4 and 1.5–1.0 m. Re-analysis of organic carbon isotope data, which are at a lower resolution, yields similar results to Storm *et al.* (2020) with power concentrated at 33–30, 14, and 5 m (>99.9% CL), and 2.4 m (>95% CL). No significant cycles were identified below the 2.4 m wavelength. Despite the lower resolution, the results from analysis of the $\delta^{13}C_{org}$ and Ca data are comparable at long periods.

Based upon average sedimentation rates and bundling of C2 and C3 cycles identified in visual analysis, the wavelengths 6.7–7.6 m are candidates for the 100-kyr eccentricity cycle, with C1 cycles therefore indicative of the 405-kyr eccentricity cycles. Thus, assuming Milankovitch ratios apply, and that the 32–24 m cycle represents the long eccentricity forcing, the 7.5–6.7, 2.4 and 1.5–1.0 m peaks align well with the predicted short eccentricity, obliquity, and orbital precession bands of the Jurassic (Waltham, 2015).

Bandpass filters (32–24 m) of the Ca and $\delta^{13}C_{org}$ data define 17.5 candidate 405 kyr cycles (Fig. 5); however, the bandpass falls out of phase with the data at 1655–1630, 1525–1490 and 1250–1280 mbs. Detailed visual analysis through the section defines between 17 and 18 cycles in total with some uncertainty at 1650 and 1390 mbs with potentially truncated cycles indicated by shorter wavelengths. Hence, taking into account the uncertainty, the Sinemurian of the Mochras borehole contains between 17 and 18 candidate 405 kyr cycles equating to an estimated floating duration of 17.5 × 405 kyr = 7090 ±200 kyr.

Tuning to the bandpass filter (32–24 m) and the custom age model from visual analysis yield consistent results, with

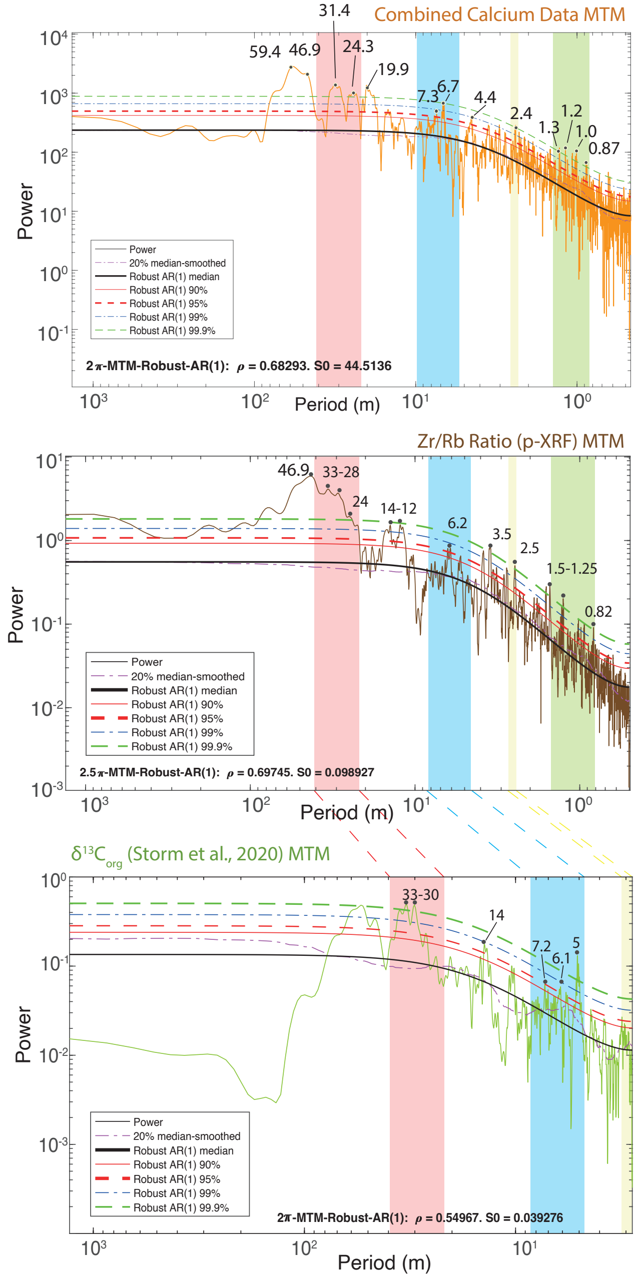

Fig. 7. MTM power spectra for the Mochras geochemical records (Ca, Zr/Rb) and $\delta^{13}C_{org}$ showing consistently power at wavelengths 33–24, 5,0–7.3 and 0.82–1.50 m

power concentrated at periodicities of 405, 100, 35 and 21–17 kyr compatible with the hypothesis of Milankovitch cyclicity. For comparison, a recent Bayesian inversion of 34 cyclostratigraphic datasets from 0–650 Ma (that includes the Pliensbachian Mochras Ca record of Ruhl *et al.*, 2016) models obliquity and precession periods at 195 Ma (Tables S3–S5, Wu *et al.*, 2024): 37.0091 ±0.2183 kyr (main obliquity period); 22.3267 ±0.0680 kyr, 21.1637 ±0.0612 kyr, and 18.2383 ±0.0477 kyr (the three main precession periods).

Further, broad peaks are present at low periods particularly at ~1.2–0.9 Myr (Fig. 8). Peaks observed at periodicities of 739 kyr and 58.8 kyr may be associated with orbital eccentricity terms (690 kyr and 54–55 kyr in figure 4.4 in Laskar, 2020).

DISCUSSION

A NEW SINEMURIAN ATS

The Mochras borehole preserves a relatively complete Sinemurian stratigraphy and, supported with data from Robin's Bay, we use Mochras as the primary basis for an assessment of the duration of the Sinemurian stage. The close agreement in number and pattern of cyclicity, primarily the interpreted 405 kyr metronome in Ca and $\delta^{13}C_{org}$ between the Cardigan Bay and Cleveland basins, is strong evidence for a larger scale climatic control on the Sinemurian marine deposits.

The high-resolution chemostratigraphy in the present study facilitates a detailed visual analysis which for the first time allows for identification of the precession band cyclicity in much of the Sinemurian. The overall interpretation here is similar to that of Storm *et al*. (2020) seen in Figure 5, with the bandpass filter used to tune the Storm model shown in grey compared to the filter used in this study in red. Our new age model yields greater time in the Bucklandi, Semicostatum, and Raricostatum zones compared to Storm *et al*. (2020) with narrowly less time in the Turneri and Oxynotum

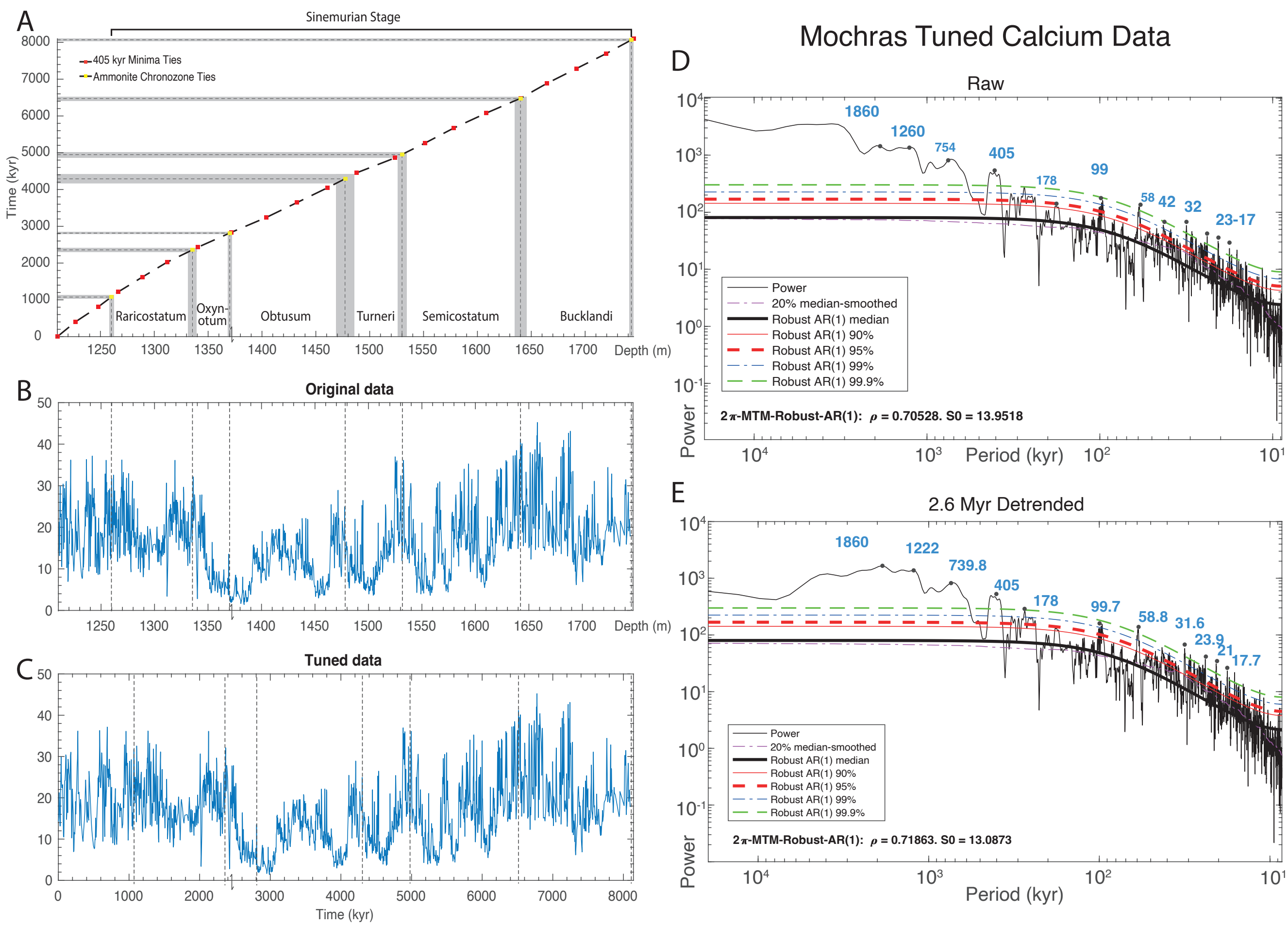

Fig. 8. Tuned Mochras calcium data

A. Time-depth plot showing age model tie points [red squares] based on tuning with the interpreted 405 kyr cycles. **B.** Tuned and **C.** untuned data, with ammonite chronozone boundaries marked using dashed lines; X-axis in C. is in time relative to top of dataset. MTM power spectra for the tuned data: **D.** raw tuned dataset, **E.** is 2.6 Myr detrended series

Zones. Storm *et al*. (2020) noted a possible shift in sedimentation rates in the Raricostatum Zone based on Evolutive Harmonic Analysis, but this change was not captured in their 405 kyr tuning, accounting for ~350 kyr of the additional time.

In addition, correlation of the new ATS for Mochras to the new astrochronology from the Sinemurian–Pliensbachian boundary section at Robin Hood's Bay, Yorkshire (Hudson *et al*., 2025), confirms the presence of 3.5 × 405 kyr cycles (~1400 kyr) in the Raricostatum Zone (Fig. 9). The Oxynotum Zone at Robin Hood's Bay has been shown to be approximately 2 × 405 kyr, or ~0.8 Myr in duration (Hudson *et al*., 2025), about 200 kyr longer than estimated here for the Mochras record (1.5 × 405 kyr cycles, or ~600 kyr), accounted for here by fault removal of the bottom part of the zone at Mochras. If this is correct, the total Sinemurian duration should be extended from 7.1 to 7.3 Myr.

Recently, Leu *et al*. (2024) have carried out a cycle analysis for the International Continental Scientific Drilling Program (ICDP) borehole drilled at Prees in the Cheshire Basin (about halfway between Mochras and Robin Hood's Bay (Fig. 1; Hesselbo *et al*., 2023). The upper Sinemurian at Prees is complicated by shallow water sedimentation and likely hiatuses, but study of the downhole gamma ray log yielded a length for the Bucklandi Zone of 1.2, and 2.4 Myr for the Semicostatum Zone. Initial results from Prees are likely to be subject to revision based on analysis of all the data, but the apparently longer duration of the Semicostatum Zone in Prees (2.4 Myr) compared to Mochras (1.6 Myr) suggests that the Bucklandi–Semicostatum interval should be the focus of more detailed study.

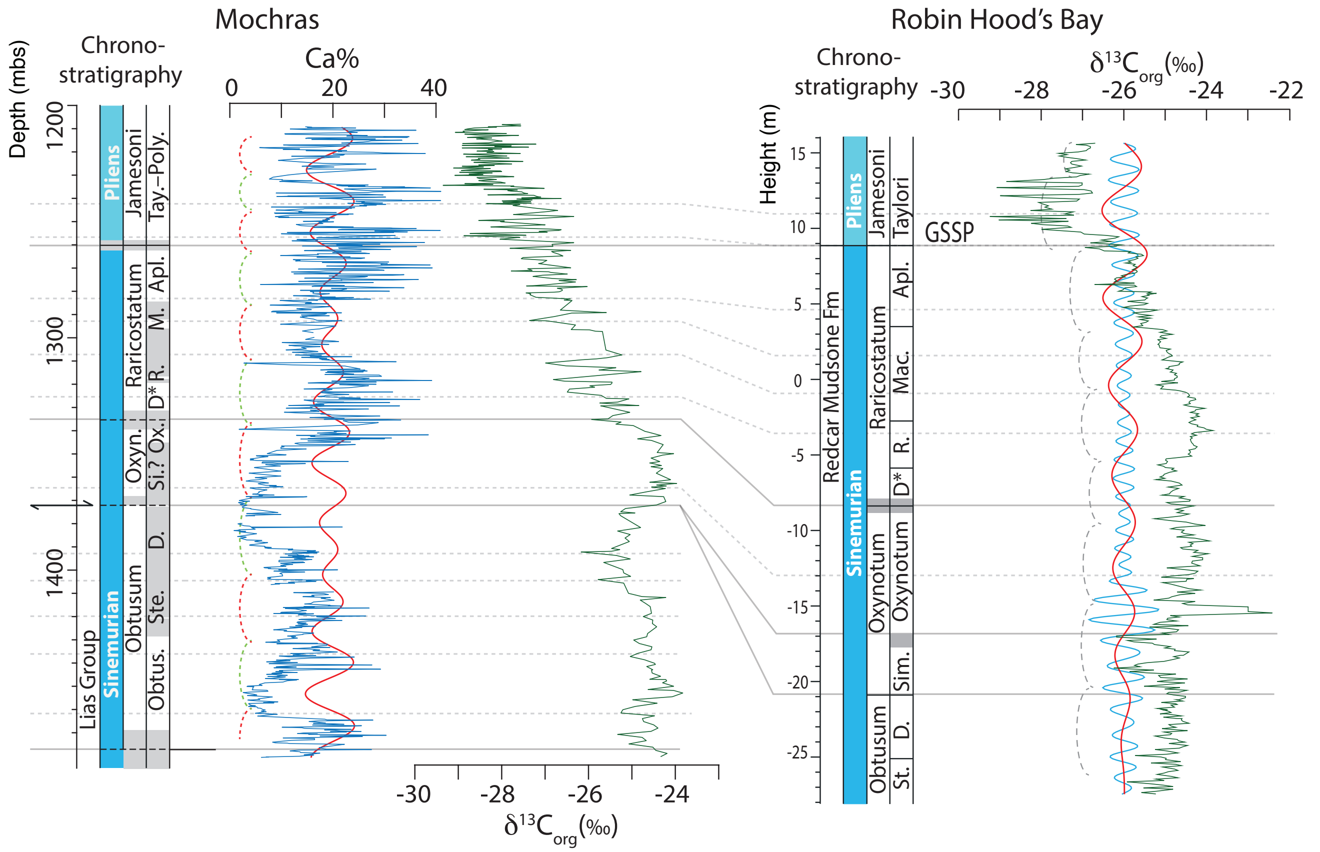

Fig. 9. Correlation of Mochras and Robin Hood's Bay based on carbon-isotope stratigraphy and ammonite chronostratigraphy

Grey shading illustrates where lack of index ammonites results in uncertain relative age assignment. Ca content records are also shown for Mochras, but the carbonate content is generally low at Robin Hood's Bay and is not shown. Interpreted 405 kyr bandpass filters (in the depth domain) are shown in red for each record along with visually identified cycles that support the bandpass filter method. Interpreted 100 kyr cycles are shown in blue for Robin Hood's Bay. Bandpass filters for Mochras are from Ca content, whilst for Robin Hood's Bay they are based on bulk organic carbon isotope stratigraphy (Hudson *et al*., 2025). Correlatable features of the carbon-isotope stratigraphy are shown using dashed grey lines, and zonal biochronostratigraphy using solid grey lines. The negative carbon isotope excursion in organic matter that characterises the Liasidium Event (lower Oxynotum Zone) at Robin Hood's Bay is cut out by the fault in Mochras at 1372 m

ACCOMMODATING TIME IN THE EARLY JURASSIC

The time available for the Sinemurian is constrained by the durations of the bounding stages (Hettangian and Pliensbachian). This is typically a good measure of whether a floating timescale is plausible. However, for the Early Jurassic there is debate surrounding the duration of the Hettangian.

The Hettangian duration has hitherto been estimated through astronomically tuned age models from St Audrie's Bay (shallow marine; Ruhl *et al*., 2010; Hüsing *et al*., 2014), the Newark–Hartford Basin astrochronstratigraphic polarity timescale (lacustrine; Kent, Olsen, 2008; Kent *et al*., 2017), and the Junggar Basin (fluvio-lacustrine; Sha *et al*., 2015) that have indicated a consistent ~1.9 Myr duration, tied to the Triassic–Jurassic boundary U-Pb age of 201.4 Ma (Schaltegger *et al.*, 2008; Schoene *et al*., 2010; Guex *et al*., 2012; Wotzlaw *et al.*, 2014). This duration is supported by correlation to a Peruvian radioisotopic (U-Pb) date of 199.4 ±0.1 Ma for the Hettangian–Sinemurian boundary (Guex *et al.*, 2012; Wotzlaw *et al*., 2014). Support for a short duration also comes from interpretations of long-term cyclic changes in palynological content from the Schandelah-1 core in Germany (Bos *et al*., 2024).

However, reinterpretation of the St Audrie's Bay succession and comparison to the adjacent Glamorgan coast, Lyme Regis (Wessex Basin) and UK Midlands successions yielded a much longer duration for the Hettangian stage (Weedon *et al*., 2018, 2019). The minimum duration for the Hettangian proposed by these authors is 4.1 Myr, obtained by taking the greatest zonal duration from each site and quantifying sometimes cryptic hiatuses using high-resolution ammonoid biohorizonal correlations (see Page, 2017 for discussion of the methodology). The amount of time suggested for St Audrie's Bay alone amounts to 3.2 Myr using the method of Weedon *et al*. (2019), meaning that even the shorter suggested duration conflicts with the Hettangian-Sinemurian boundary age of 199.4 ±0.1 Myr (Guex *et al*., 2012; Wotzlaw *et al*., 2014). On the other hand, the ash bed in which that age is measured is located within a 13 m biostratigraphic gap between the last Hettangian specimen and the first Sinemurian indicator (Weedon *et al.*, 2019). With this much biostratigraphic uncertainty the true uncertainty associated with the boundary age is far greater than quantified and should be treated as provisional until further data are available.

To evaluate the longer duration, it is necessary to understand which part of the SW UK succession the additional time of Weedon *et al.* (2019) comes from. The study of Ruhl *et al*. (2010) notably did not include the Tilmanni Zone at the base of the Jurassic, and the Weedon *et al*. (2019) added ~530 kyr based on estimated length of this zone. The Weedon *et al*. (2019) study also added a further 730 kyr through interpretation of much lower sedimentation rates in the Planorbis Zone, arguing that a sedimentary cyclicity at ~70 cm wavelength is not precession-controlled at St Audrie's Bay or in Glamorgan, as implied by Ruhl *et al*. (2010), but instead a product of short eccentricity forcing. Weedon *et al*. (2019) argue that the bed thicknesses in the Planorbis Zone are evidence for a very slow sedimentation rate. They also suggested that the irregular spacing stemming from omission of limestone beds in the analysis of Ruhl *et al.* (2010), resulted in missed shorter period cycles and incorrect cycle assignment. Although it is undoubtably correct that the 1.7 Myr from St Audrie's Bay is an underestimation, re-analysis of Ruhl *et al*. (2010) data with inclusion of limestones, and accounting for the Tilmanni Zone, produced a 1.97 Myr duration (Huang, 2018), and also identified precession and obliquity band cyclicity above the 95% CL in the periods predicted by Ruhl *et al*. (2010).

The remaining additional time is related to the integration and correlation of ammonite bio-horizons into the astronomical models. The Weedon *et al.* (2019) interpretation is based on systematic cm-by-cm collection of ammonoids from all three key sections (Lyme Regis, West Somerset coast, and Lavernock) and recovery of over 3500 specimens. The identified Biohorizons were used to provide chronostratigraphic tie-lines between sections (Weedon *et al*., 2018, 2019). As discussed by Weedon *et al.* (2018) clustering of biohorizons records in one section relative to another provides evidence of slowed sedimentation including potential hiatuses, but the absence of a record can also be due to other factors including preservational. Confirmation of the nature of any apparent gaps – and hence 'missing' cycles in any section – would, however, require further investigation (see *e.g.*, Ullmann *et al.*, 2025 for example of complementary chemostratigraphic approach).

On balance, it is difficult to resolve the two estimates (1.9 Myr versus 4.1 Myr) for the duration of the Hettangian based only on the existing data. The methodology presented by Weedon *et al*. (2019) using multiple sites and assuming maximum incompleteness at each site will *a priori* create long timescales, whilst the contrasting assumption of default section completeness will tend to produce timescales that are too short. The true duration is likely to lie between these end members.

Assuming a 'short' duration for the Hettangian (~2 Myr), the 7.3 Myr duration estimate for the Sinemurian herein is within error of the current time available for the Sinemurian based on radio-isotopic tie-points and previous estimated durations for the Pliensbachian Stage (Fig. 10). However, more than ~0.5 Myr additional time added to the Hettangian or the Sinemurian creates a problem that requires accommodation. For example, a 4.1 Myr long Hettangian would leave only 4.9 Myr for the Sinemurian (Weedon *et al*., 2019). The base-Hettangian (Triassic–Jurassic) boundary has a highly reproducible robust age that prevents significant additional Hettangian/Sinemurian time being added at the base of the Jurassic (*e.g.* as summarised in Hesselbo *et al*., 2020a).

Additional time could also hypothetically be removed from the Pliensbachian to Toarcian interval. The base-Pliensbachian boundary at 192.5 ±0.4 Myr is not constrained through firm radiometric dating and comes from the 8.4–8.9 Myr astronomically tuned age model for the Pliensbachian of the Mochras borehole, which has a clear 405-kyr cyclicity, and high-resolution calcium content and $\delta^{13}C_{org}$ data as well as corroborating data from ichnofossils and facies analysis (Ruhl *et al*., 2016; Huang, 2018; Hesselbo *et al*., 2020c; Storm *et al*., 2020; Pieńkowski *et al*., 2021; Hollaar *et al*., 2024). A similar duration (8.7 Myr) was also calculated recently based on analysis of a magnetic susceptibility record from the Sancerre Borehole, Paris Basin, France (Charbonnier *et al*., 2023). The Mochras record is tied to the base-Toarcian radiometric age of 183.5 ±0.5 Myr in Argentina (refined from Al-Suwaidi *et al*. (2022) using carbon-isotope stratigraphy for precise correlation to the GSSP). It is possible that correlation uncertainty here could accommodate some time because correlation with European sections is based on a combination of carbon-isotope stratigraphy and ammonite biostratigraphy, but an increasing abundance of data (*e.g.*, Storm *et al*., 2024) supports the correlation.

Further correlatable and precisely dated horizons also exist from the late Pliensbachian of the western US (De Lena *et al.*, 2019) and for the Toarcian Oceanic Anoxic Event in Japan (Kemp *et al.*, 2024). As shown in Figure 10, even the end of the Toarcian Oceanic Anoxic Event becomes Pliensbachian in age with a 'long' Hettangian and assuming the Sinemurian estimate presented here is correct, whilst the definite late Pliensbachian tie point becomes 'early-mid Pliensbachian' in age. Such distortions of the time scale are inadmissible.

In summary, the longer Sinemurian is within error of the time available to accommodate it only by accepting a 'short' Hettangian. This observation suggests that the longest duration of 4.1 Myr proposed for the Hettangian by Weedon *et al.* (2019) is too long, due to perhaps minor uncertainties in the biohorizon method, but likely mostly related to overestimation of the time allocated to the basal two zones of the stage. It is also possible that any additional time, if present, could be accounted for by a shortened Pliensbachian, but this alternative solution conflicts with an increasing number of other studies.

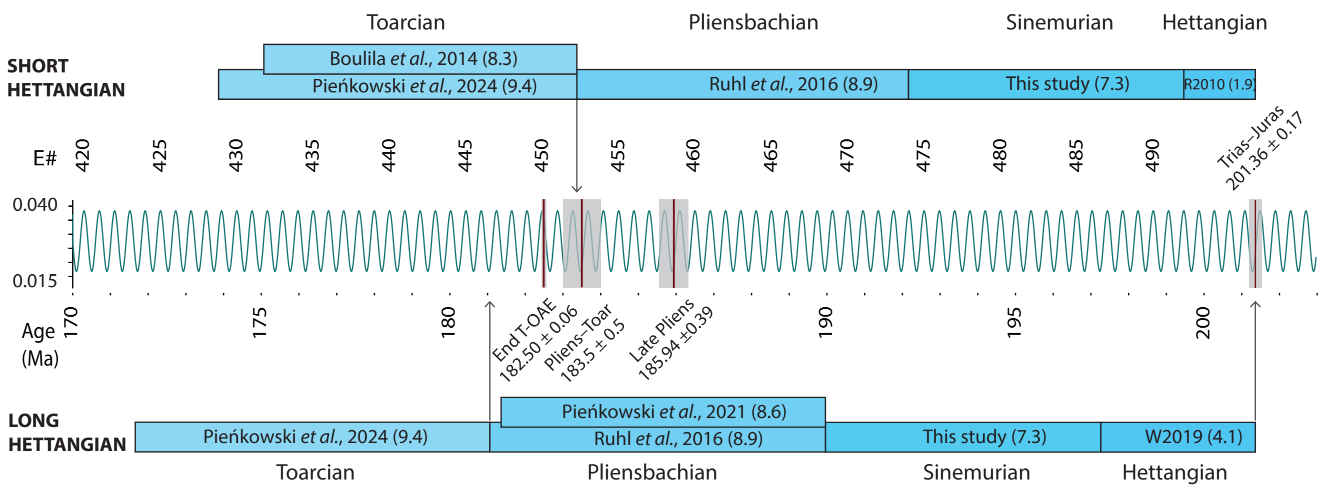

Fig. 10. Schematic figure showing implications of the length of the Sinemurian for the length of the Hettangian and compatibility with published radioisotopic ages

The radioisotopic constraints are as follows: End T-OAE, U-Pb, 182.50 ±0.06 Ma (Kemp *et al*., 2024); Base Toarcian, U–Pb, 183.5 ±0.5 Ma (adjusted from Al-Suwaidi *et al.* (2022) to accommodate correlation between Neuquén Basin, Argentina and UK sections based on carbon-isotope stratigraphy rather than first occurrence of *Dactylioceras* (*Eodactylioceras*) *simplex*; Start of Late Pliensbachian Event, U–Pb, 185.94 ±0.39 Ma (De Lena *et al*., 2019); Base Hettangian (Triassic–Jurassic boundary), U-Pb, 201.36 ±0.17 Ma (Wotzlaw *et al*., 2014). Stage durations are from the following sources: Toarcian, Mochras, Pieńkowski *et al.* (2024); Toarcian, Sancerre, Paris Basin, Boulila *et al.* (2014); Pliensbachian, Mochras, Ruhl *et al.* (2016), Pieńkowski *et al.* (2021); Sinemurian, this study; Hettangian, Weedon *et al.* (2019), Ruhl *et al.* (2010). Long-eccentricity curve assumes 405 kyr period, calculated and numbered from present day orbital state (Laskar, 2020)

CONCLUSIONS

The geochemical and geophysical datasets generated for the Sinemurian and earliest Pliensbachian of the Mochras borehole exhibit a full suite of Milankovitch periodicities identified through power spectral analysis. The stable 405-kyr eccentricity cycle is dominant in carbon-isotope and elemental data, reflecting periodic changes in the depositional environment. Using the 405-kyr metronome, the amount of time recorded in the Mochras boreholes is re-estimated. Approximately ~0.2 Myr of record is suggested to be missing at Mochras due to intersection of the borehole with an extensional fault. Primarily using the high-resolution Ca-content data for the expanded Mochras succession, a detailed astronomically tuned timescale is constructed for the Sinemurian stage, suggesting 7.3 Myr duration for the whole stage. Based on radioisotopic constraints and previous studies of the Pliensbachian duration, a short (~ 2 Myr) Hettangian is deemed most likely correct.

Acknowledgements. AJLH acknowledges PhD studentship funding from the Natural Environment Research Council (NERC) GW4+, Doctoral Training Partnership (DTP) (NE/L002434/1), and the British Geological Survey (Contract GA/16S/018). SPH and CVU acknowledge NERC grant (NE/N018508/1) and funding from the International Continental Scientific Drilling Program (ICDP) for the JET project (Integrated Understanding of the Early Jurassic Earth System and Timescale). JBR publishes with the approval of the Director, British Geological Survey (NERC). LAH thanks the Heising-Simons Foundation for their support through Grant No. 2021-2796. Staff at the BGS National Geological Repository, British Geological Survey, Keyworth, are warmly thanked for their longstanding support. We are grateful to reviewers Jozsef Pálfy and Mathieu Martinez for their insightful comments.

We dedicate this article to Professor Grzegorz Pieńkowski.

REFERENCES

AL-SUWAIDI A.H., RUHL M., JENKYNS H.C., DAMBORENEA S.E., MANCEÑIDO M.O., CONDON D.J., ANGELOZZI G.N., KAMO S.L., STORM M., RICCARDI A.C., HESSELBO S.P., 2022 – New age constraints on the Lower Jurassic Pliensbachian – Toarcian Boundary at Chacay Melehue (Neuquén Basin, Argentina). *Scientific Reports*, **12**: 4975. https://doi.org/10.1038/s41598-022-07886-x.

ARKELL W.J., 1933 – The Jurassic System in Great Britain. Clarendon Press, Oxford.

ARKELL W.J., 1956 – Jurassic Geology of the World. Oliver and Boyd Ltd, Edinburgh.

BJERRUM C.J., SURLYK F., CALLOMON J.H., SLINGERLAND R.L., 2001 – Numerical paleoceanographic study of the Early Jurassic transcontinental Laurasian Seaway. *Paleoceanography*, **16**: 390–404. https://doi.org/10.1029/2000PA000512.

BLOOS G., PAGE K.N., 2002 – Global stratotype section and point for base of the Sinemurian Stage (Lower Jurassic). *Episodes*, **25**: 22–28.

BONIS N.R., RUHL M., KÜRSCHNER W.M., 2010 – Milankovitch-scale palynological turnover across the Triassic–Jurassic transition at St. Audrie's Bay, SW UK. *Journal of the Geological Society of London*, **16**: 877–888. https://doi.org/10.1144/0016-76492009-141.

BOS R., ZHENG W., LINDSTRÖM S., SANEI H., WAAJEN I., FENDLEY I.M., MATHER T.A., WANG Y., ROHOVEC J., NAVRÁTIL T., SLUIJS A., van de SCHOOTBRUGGE B., 2024 – Climate-forced Hg-remobilization associated with fern mutagenesis in the aftermath of the end-Triassic extinction. *Nature Communications*, **15**, 3596. https://doi.org/10.1038/s41467-024-47922-0.

BOULILA S., GALBRUN B., HURET E., HINNOV L.A., ROUGET I., GARDIN S., BARTOLINI A., 2014 – Astronomical calibration of the Toarcian Stage: implications for sequence stratigraphy and duration of the early Toarcian OAE. *Earth and Planetary Science Letters*, **386**: 98–111. https://doi.org/10.1016/j.epsl.2013.10.047.

BURGESS S.D., BOWRING S.A., FLEMING T.H., ELLIOT D.H., 2015 – High-precision geochronology links the Ferrar large igneous province with early-Jurassic ocean anoxia and biotic crisis. *Earth and Planetary Science Letters*, **415**: 90–99. https://doi.org/10.1016/j.epsl.2015.01.037.

CARUTHERS A.H., SMITH P.L. GRÖCKE D.R., 2013 – The Pliensbachian–Toarcian (Early Jurassic) extinction, a global multi-phased event. *Palaeogeography, Palaeoclimatology, Palaeoecology*, **386**: 104–118. https://doi.org/10.1016/j.palaeo.2013.05.010.

CECCA F., MACCHIONI F., 2004 – The two Early Toarcian (Early Jurassic) extinction events in ammonoids. *Lethaia*, **37**: 35–56. https://doi.org/10.1080/00241160310008257.

CHARBONNIER G., BOULILA S., GALBRUN B., LASKAR J., GARDIN S., ROUGET I., 2023 – A 20-million-year Early Jurassic cyclostratigraphic record and its implications for the chaotic inner Solar System and sea-level changes. *Basin Research*, **35**: 1288–1307. https://doi.org/10.1111/bre.12754.

CLÉMENCE M.-E., BARTOLINI A., GARDIN S., PARIS G., BEAUMONT V., PAGE K.N., 2010 – Early Hettangian benthic–planktonic coupling at Doniford (SW England): Palaeoenvironmental implications from the aftermath of the end-Triassic crisis. *Palaeogeography, Palaeoclimatology, Paleoecology*, **295**: 102–115. https://doi.org/10.1016/j.palaeo.2010.05.021.

COHEN A.S., COE A.L., 2002 – New geochemical evidence for the onset of volcanism in the Central Atlantic magmatic province and environmental change at the Triassic–Jurassic boundary. *Geology*, **30**: 267–270. https://doi.org/10.1130/0091-7613(2002)030<0267:NGEFTO>2.0.CO;2.

COPE J.C.W., GETTY T.A., HOWARTH M.K., MORTON N., TORRENS H.S., 1980 – A correlation of Jurassic rocks in the British Isles. Part One: Introduction and Lower Jurassic. *Geological Society London, Special Report*, **14**: 1–73.

COPE J.C.W., INGHAM J.K., RAWSON P.F. (Eds.), 1992 – Atlas of Palaeogeography and Lithofacies. *Geological Society Memoir*, **13**: 1–164.

COPESTAKE P., JOHNSON B., 2014 – Lower Jurassic Foraminifera from the Llanbedr (Mochras Farm) Borehole, North Wales, UK. *Monograph of the Palaeontonographical Society*, **167**, 641: 1–403. https://doi.org/10.1080/02693445.2013.11963952.

COX B.M., 1990 – A review of Jurassic chronostratigraphy and age indicators for the UK. *In*: Events responsible for Britain's oil and gas reserves (Eds. R.F.P. Hardman, J. Brooks). *Geological Society of London, Special Publication*, **55**: 169–190. https://doi.org/10.1144/GSL.SP.1990.055.01.08.

COX B.M., SUMBLER M.G., IVIMEY-COOK H.C., 1999 – A formational framework for the Lower Jurassic of England and Wales (onshore area). *British Geological Survey Research Report*, **RR/99/01**: 1–28.

DAVIES J.H.F.L., MARZOLI A., BERTRAND H., YOUBI N., ERNESTO M., SCHALTEGGER U., 2017 – End-Triassic mass extinction started by intrusive CAMP actsivity. *Nature Communications*, **8**: 15596. https://doi.org/10.1038/ncomms15596.

DEAN W.T., DONOVAN D.T., HOWARTH M.K., 1961 – The Liassic ammonite zones and subzones of the north-west European Province. *Bulletin of the British Museum (Natural History) Geology Series*, **4**: 435–505.

DE LENA L., TAYLOR D., GUEX, J., BARTOLINI A., ADATTE T., van ACKEN D., SPANGENBERG J.E., SAMANKASSOU E., VENNEMANN T., SCHALTEGGER U., 2019 – The driving mechanisms of the carbon cycle perturbations in the late Pliensbachian (Early Jurassic). *Scientific Reports*, **9**: 18430. https://doi.org/10.1038/s41598-019-54593-1.

DOBSON M.R., WHITTINGTON R.J., 1987 – The geology of Cardigan Bay. *Proceedings of the Geologists' Association*, **98**: 331–353. https://doi.org/10.1016/S0016-7878(87)80074-3.

DUARTE L.V., COMAS-RENGIFO M.J., SILVA R.L., PAREDES R., GOY A., 2014 – Carbon isotope stratigraphy and ammonite biochronostratigraphy across the Sinemurian–Pliensbachian boundary in the western Iberian margin. *Bulletin of Geosciences*, **89**: 719–736. https://doi.org/10.3140/bull.geosci.1476.

FENDLEY I.M., FRIELING J., MATHER T.A., RUHL M., HESSELBO S.P., JENKYNS H.C., 2024 – Quantifying Early Jurassic Large Igneous Province carbon emissions via sedimentary mercury. *Nature Geoscience*, **17**: 241–248. https://doi.org/10.1038/s41561-024-01378-5.

FRANCESCHI M., DAL CORSO J., POSENATO R., ROGHI G., MASETTI D., JENKYNS H.C., 2014 – Early Pliensbachian (Early Jurassic) C-isotope perturbation and the diffusion of the Lithiotis Fauna: Insights from the western Tethys. *Palaeogeography, Palaeoclimatology, Palaeoecology*, **410**: 255–263. https://doi.org/10.1016/j.palaeo.2014.05.025.

GAMBACORTA G., BRUMSACK H.-J., JENKYNS H.C., ERBA E., 2024 – The early Toarcian Oceanic Anoxic Event (Jenkyns Event) in the Alpine-Mediterranean Tethys, north African margin, and north European epicontinental seaway. *Earth-Science Reviews*, **248**: 104636. https://doi.org/10.1016/j.earscirev.2023.104636.

GUEX J., SCHOENE B., BARTOLINI A., SPANGENBERG J., SCHALTEGGER U., O'DOGHERTY L., TAYLOR D., BUCHER H., ATUDOREI V., 2012– Geochronological constraints on post-extinction recovery of the ammonoids and carbon cycle perturbations during the Early Jurassic. *Palaeogeography, Palaeoclimatology, Palaeoecology*, **346**: 1–11. https://doi.org/10.1016/j.palaeo.2012.04.030.

HALLAM A., 2001 – A review of the broad pattern of Jurassic sea-level changes and their possible causes in the light of current knowledge. *Palaeogeography, Palaeoclimatology, Palaeoecology*, **167**: 23–37. https://doi.org/10.1016/S0031-0182(00)00229-7.

HEIMDAL T.H., JONES M.T., SVENSEN H.H., 2020 – Thermogenic carbon release from the Central Atlantic magmatic province caused major end-Triassic carbon cycle perturbations. *Proceedings of the National Academy of Sciences*, **117**: 11968–11974. https://doi.org/10.1073/pnas.2000095117.

HESSELBO S.P., 2012 – Late Triassic–Jurassic: Disintegrating Pangaea. *In*: Geological History of Britain and Ireland (Second Edition) (Eds. N.H. Woodcock, R.A. Strachan). Blackwell, Oxford.

HESSELBO S.P., JENKYNS H.C., 1995 – A comparison of the Hettangian to Bajocian successions of Dorset and Yorkshire. *In*: Field Geology of the British Jurassic (Ed. P.D. Taylor): 105–150. The Geological Society of London.

HESSELBO S.P., GRÖCKE D.R., JENKYNS H.C., BJERRUM C.J., FARRIMOND P.L., MORGANS-BELL H.S., GREEN O., 2000 – Massive dissociation of gas hydrates during a Jurassic Oceanic Anoxic Event. *Nature*, **406**: 392–395. https://doi.org/10.1038/35019044.

HESSELBO S.P., ROBINSON S.A., SURLYK F., PIASECKI S., 2002 – Terrestrial and marine extinction at the Triassic-Jurassic boundary synchronized with major carbon-cycle perturbation: a link to initiation of massive volcanism? *Geology*, **30**: 251–254. https://doi.org/10.1130/0091-7613(2002)030<0251:TAMEAT>2.0.CO;2.

HESSELBO S.P., JENKYNS H.C., DUARTE L.V., OLIVEIRA L.C.V., 2007 – Carbon-isotope record of the Early Jurassic (Toarcian) Oceanic Anoxic Event from fossil wood and marine carbonate (Lusitanian Basin, Portugal). *Earth and Planetary Science Letters*, **253**: 455–470. https://doi.org/10.1016/j.epsl.2006.11.009.

HESSELBO S.P., BJERRUM C.J., HINNOV L.A., MACNIOCAILL C., MILLER K.G., RIDING J.B., van de SCHOOTBRUGGE B., and the Mochras Revisted Science Team, 2013 – Mochras borehole revisited: A new global standard for Early Jurassic earth history. *Scientific Drilling*, **16**: 81–91. https://doi.org/10.5194/sd-16-81-2013.

HESSELBO S.P., KORTE C., ULLMANN C.V., EBBESEN A., 2020a – Carbon and oxygen isotope records from the southern Eurasian Seaway following the Triassic–Jurassic boundary: parallel long-term enhanced carbon burial and seawater warming. *Earth-Science Reviews*, **203**: 103131. https://doi.org/10.1016/j.earscirev.2020.103131.

HESSELBO S.P., HUDSON A.J.L., HUGGETT J.M., LENG M.J., RIDING J.B., ULLMANN C.V., 2020b – Palynological, geochemical, and mineralogical characteristics of the Early Jurassic Liasidium Event in the Cleveland Basin, Yorkshire, UK. *Newsletters on Stratigraphy*, **53**: 191–211. https://doi.org/10.1127/nos/2019/0536.

HESSELBO S.P., OGG J.G., RUHL M., 2020c – The Jurassic Period. *In*: Geologic Time Scale 2020 (Eds. F.M., Gradstein *et al.*): 955–1021. Elsevier. https://doi.org/10.1016/B978-0-12-824360-2.00026-7.

HESSELBO S.P., and 72 others, 2023 – Initial results of coring at Prees, Cheshire Basin, UK (ICDP JET Project); towards an integrated stratigraphy, timescale, and Earth system understanding for the Early Jurassic. *Scientific Drilling*, **32**: 1–25. https://doi.org/10.5194/sd-32-1-2023.

HOLLAAR T.P., BAKER S.J., HESSELBO S.P., DECONINCK J.-F., MANDER L., RUHL M., BELCHER C.M., 2021 – Wildfire activity enhanced during phases of maximum orbital eccentricity and precessional forcing in the Early Jurassic. *Communications Earth & Environment*, **2**: 247. https://doi.org/10.1038/s43247-021-00307-3.

HOLLAAR T.P., HESSELBO S.P., DECONINCK J.-F., DAMASCHKE M., ULLMANN C.V., JIANG M., BELCHER C.M., 2023 – Environmental changes during the onset of the Late Pliensbachian Event (Early Jurassic) in the Cardigan Bay Basin, Wales. *Climate of the Past*, **19**: 979–997. https://doi.org/10.5194/cp-19-979-2023.

HOLLAAR T.P., BELCHER C.M., RUHL M., DECONINCK J.-F., HESSELBO S.P., 2024 – The optimum fire window: Applying the fire-productivity hypothesis to Jurassic climate states. *Biogeosciences*, **21**: 2795–2809. https://doi.org/10.5194/bg-21-2795-2024.

HUANG C., 2018 – Astronomical time scale for the Mesozoic. *In*: Stratigraphy & Timescales (Ed. M. Montannari), **3**: 81–150. Academic Press. https://doi.org/10.1016/bs.sats.2018.08.005.

HUDSON A.J.L., 2021 – Magnitude and pacing of Early Jurassic palaeoclimate change: Chemostratigraphy and cyclostratigraphy of the British Lower Jurassic (Sinemurian–Pliensbachian) [Unpublished PhD thesis]. University of Exeter.

HUDSON A.J.L., ULLMANN C.V., HINNOV L.A., PAGE K.N., HESSELBO S.P., 2025 – Integrated astrochronology, sequence stratigraphy, and chronostratigraphy in shallow marine mudrocks (Lower Jurassic, Cleveland Basin, UK). *Sedimentologika*, **3**. https://doi.org/10.57035/journals/sdk.2025.e31.1240.

HÜSING S.K., BENIEST A., van der BOON, A., ABELS, H.A., DEENEN M.H.L., RUHL M., KRIJGSMAN W., 2014 – Astronomically-calibrated magnetostratigraphy of the Lower Jurassic marine successions at St. Audrie's Bay and East Quantoxhead (Hettangian–Sinemurian; Somerset, UK). *Palaeogeography, Palaeoclimatology, Palaeoecology*, **403**: 43–56. https://doi.org/10.1016/j.palaeo.2014.03.022.

IKEDA M., TADA R., 2014 – A 70 million year astronomical time scale for the deepsea bedded chert sequence (Inuyama, Japan): Implications for Triassic–Jurassic geochronology. *Earth and Planetary Science Letters*, **399**: 30–43. https://doi.org/10.1016-/j.epsl.2014.04.031.

JENKYNS H.C., 1988 – The early Toarcian (Jurassic) anoxic event: Stratigraphic, sedimentary and geochemical evidence. *American Journal of Science*, **288**: 101–151.

JENKYNS H.C., 2010 – Geochemistry of oceanic anoxic events. *Geochemistry, Geophysics, Geosystems*, **11**, Q03004. https://doi.org/10.1029/2009GC002788.

JENKYNS H.C., WEEDON G.P., 2013 – Chemostratigraphy ($CaCO_3$, TOC, $\delta^{13}C_{org}$) of Sinemurian (Lower Jurassic) black shales from the Wessex Basin, Dorset and palaeoenvironmental implications. *Newsletters on Stratigraphy*, **46**: 1–21. https://doi.org/10.1127/0078-0421/2013/0029.

JENKYNS H.C., JONES C.E., GRÖCKE D.R., HESSELBO S.P., PARKINSON D.N., 2002 – Chemostratigraphy of the Jurassic System: Applications, limitations and implications for palaeoceanography. *Journal of the Geological Society of London*, **159**: 351–378. https://doi.org/10.1144/0016-764901-130.

KEMP D.B., COE A.L., COHEN A.S., SCHWARK L., 2005 – Astronomical pacing of methane release in the early Jurassic period. *Nature*, **437**: 396–399. https://doi.org/10.1038/nature04037.

KEMP D.B., RAMEZANI J., IZUMI K., AL-SUWAIDI A., HUANG C., CHEN W., YUQING ZHU Y. 2024 – The timing and duration of large-scale carbon release in the Early Jurassic. *Geology*, **52**: 891–895. https://doi.org/10.1130/G52457.1.

KENT D.V., OLSEN P.E., 2008 – Early Jurassic magnetostratigraphy and paleolatitudes from the Hartford continental rift basin (eastern North America): Testing for polarity bias and abrupt polar wander in association with the central Atlantic magmatic province. *Journal of Geophysical Research: Solid Earth,* **113**: B06105. https://doi.org/10.1029/2007JB005407.

KENT D.V., OLSEN P.E., MUTTONI G., 2017 – Astrochronostratigraphic polarity time scale (APTS) for the Late Triassic and Early Jurassic from continental sediments and correlation with standard marine stages. *Earth-Science Reviews*, **166**: 153–180. https://doi.org/10.1016/j.earscirev.2016.12.014.

KORTE C., HESSELBO S.P., 2011 – Shallow-marine carbon- and oxygen-isotope and elemental records indicate icehouse-greenhouse cycles during the Early Jurassic. *Paleoceanography*, **26**: PA4219. https://doi.org/10.1029/2011PA002160.

KORTE C., HESSELBO S.P., JENKYNS H.C., RICKABY R.E.M., SPÖTL C., 2009 – Palaeoenvironmental significance of carbon- and oxygen-isotope stratigraphy of marine Triassic–Jurassic boundary sections in SW Britain. *Journal of the Geological Society of London*, **166**: 431–445. https://doi.org/10.1144/0016-76492007-177.

KORTE C., HESSELBO S.P., ULLMANN C.V., DIETL G., RUHL M., SCHWEIGERT G., THIBAULT N., 2015 – Jurassic climate mode governed by ocean gateway. *Nature Communications*, **6**: 10015. https://doi.org/10.1038/ncomms10015.

KORTE C., RUHL M., PÁLFY J., ULLMANN C.V., HESSELBO S.P. 2019 – Chemostratigraphy across the Triassic–Jurassic boundary. *In*: Chemostratigraphy Across Major Chronological Boundaries (Eds. A.N. Sial *et al.*). *American Geophysical Union Geophysical Monograph*, **240**: 185–210. The American Geophysical Union. John Wiley & Sons, Inc. AGU Books. https://doi.org/10.1002/9781119382508.ch10.

LAGRANGE M.T., KONHAUSER K.O., CATUNEANU O., HARRIS B.S., PLAYTER T.L., GINGRAS M.K., 2020 – Sequence stratigraphy in organic-rich marine mudstone successions using chemostratigraphic datasets. *Earth-Science Reviews*, **203**: 103137. https://doi.org/10.1016/j.earscirev.2020.103137.

LASKAR J., 2020 – Chapter 4 – Astrochronology. *In*: Geologic Time Scale (Eds. F.M. Gradstein *et al.*), **1**: 139–158. Elsevier. https://doi.org/10.1016/B978-0-12-824360-2.00004-8.

LEU K., ZEEDEN C., ULFERS A., ABADI M.S., VINNEPAND M., RUHL M., HESSELBO S.P., WONIK T., 2024 – Astronomical calibration of the Early Jurassic Sinemurian Stage based on cyclostratigraphic studies of downhole logging data in the Prees 2 borehole (England). *Newsletters on Stratigraphy*, **57**: 257–282. https://doi.org/10.1127/nos/2024/0803.

LI M., KUMP L.R., HINNOV L.A., MANN M.E., 2018 – Tracking variable sedimentation rates and astronomical forcing in Phanerozoic paleoclimate proxy series with evolutionary correlation coefficients and hypothesis testing. *Earth and Planetary Science Letters*, **501**: 165–179. https://doi.org/10.1016/j.epsl.2018.08.041.

LI M., HINNOV L., KUMP L., 2019 – Acycle: Time-series analysis software for paleoclimate research and education. *Computers & Geosciences*, **127**: 12–22. https://doi.org/10.1016/j.cageo.2019.02.011.

LINDSTRÖM S., 2021 – Two-phased mass rarity and extinction in land plant during the end-Triassic Climate Crisis. *Frontiers in Earth Sciences*, **9**: 1079. https://doi.org/10.3389/feart.2021.780343.

LITTLE C.T., BENTON M.J., 1995 – Early Jurassic mass extinction: A global long-term event. *Geology*, **23**: 495–498. https://doi.org/10.1130/0091-7613(1995)023<0495:EJMEAG>2.3.CO;2.

MEISTER C., ABERHAN M., BLAU J., DOMMERGUES J.-L., FEIST-BURKHARDT S., HAILWOOD E.A., HART M., HESSELBO S.P., HOUNSLOW M.W., HYLTON M., MORTON N., PAGE K.N., PRICE G.D., 2006 – The Global Boundary Stratotype Section and Point (GSSP) for the base of the Pliensbachian Stage (Lower Jurassic), Wine Haven, Yorkshire, UK. *Episodes*, **29**: 93–106.

MEYERS S.R., SAGEMAN B.B., 2007– Quantification of deep-time orbital forcing by average spectral misfit. *American Journal of Science*, **307**: 773–792. https://doi.org/10.2475/05.2007.01.

PAGE K.N., 2003 – The Lower Jurassic of Europe – its subdivision and correlation. *In*: The Jurassic of Denmark and Adjacent Areas (Eds. J. Ineson, F. Surlyk). *Geological Survey of Denmark and Greenland, Bulletin*, **1**: 23–59. https://doi.org/10.34194/geusb.v1.4646.

PAGE K.N., 2008 –The evolution and geography of Jurassic ammonites. *Proceedings of the Geologists' Association*, **119**: 35–57. https://doi.org/10.1016/S0016-7878(08)80257-X.

PAGE K.N., 2010a – High resolution ammonite stratigraphy of the Charmouth Mudstone Formation (Lower Jurassic: Sinemurian-Lower Pliensbachian) in south-west England (UK). *Volumina Jurassica*, **7**: 19–29.

PAGE K.N., 2010b – Stratigraphic Framework. *In*: Fossils from the Lower Lias of the Dorset Coast (Eds. A.R. Lord, P.G. Davis): 30–40. Palaeontological Association.

PAGE K.N., 2017 – From Oppel to Callomon (and beyond!): Building a high-resolution ammonite-based biochronology for the Jurassic System. *Lethaia*, **50**: 336–355. https://doi.org/10.1111/let. 12209.

PAGE K.N., OATES M.J., SIMMS M.J., EDWARDS M., 2025 – Hettangian and Sinemurian. *In*: A Correlation of Jurassic Rocks in the British Isles (second edition) (Eds. J.W.C. Cope, M.I Wakefield). In revision.

PÁLFY J, SMITH P.L., 2000 – Synchrony between Early Jurassic extinction, oceanic anoxic event, and the Karoo-Ferrar flood basalt volcanism. *Geology*, **28**: 747–750. https://doi.org/10.1130/0091-7613(2000)28<747:SBEJEO>2.0.CO;2.

PÁLFY J., MORTENSEN J.K., CARTER E.S., SMITH P.L., FRIEDMAN R.M., TIPPER H.W., 2000 – Timing of the end-Triassic mass extinction: first on land, then in the sea? *Geology*, **28**: 39–42. https://doi.org/10.1130/0091-7613(2000)28<39:TTEMEF>2.0.CO;2.

PÁLFY J., DEMÉNY A., HAAS J., HETÉNYI M., ORCHARD M.J., VETŐ I., 2001 – Carbon isotope anomaly and other geochemical changes at the Triassic–Jurassic boundary from a marine section in Hungary. *Geology*, **29**: 1047–1050. https://doi.org/10.1130/0091-7613(2001)029<1047:CIAAOG>2.0.CO;2.

PERCIVAL L.M.E., WITT M.L.I., MATHER T.A., HERMOSO M., JENKYNS H.C., HESSELBO S.P., AL-SUWAIDI A.H., STORM M.S., XU W., RUHL M., 2015 – Globally enhanced mercury deposition during the end-Pliensbachian extinction and Toarcian OAE: A link to the Karoo-Ferrar Large Igneous Province. *Earth and Planetary Science Letters*, **428**: 267–280. https://doi.org/10.1016/j.epsl.2015.06.064.

PERCIVAL L.M.E, COHEN A.S., DAVIES M.K., DICKSON A.J., HESSELBO S.P., JENKYNS H.C., LENG M.J., MATHER T.A., STORM M.S., XU W., 2016 – Osmium isotope evidence for two pulses of increased continental weathering linked to Early Jurassic volcanism and climate change. *Geology*, **44**: 759–762. https://doi.org/10.1130/G37997.1.

PHARAOH T.C., 1996 – Tectonic map of Britain, Ireland and adjacent areas. Sheet 1. 1:500,000. British Geological Survey, Keyworth, UK.

PIEŃKOWSKI G., 2004 –The epicontinental Lower Jurassic of Poland. *Polish Geological Institute Special Publication*, **12**: 1–152.

PIEŃKOWSKI G., SCHUDACK M.E., BOSÁK P., ENAY R., FELDMAN-OLSZEWSKA A., GOLONKA J., GUTOWSKI J., HERNGREEN G.F.W., JORDAN P., KROBICKI M., LATHUILIERE B., LEINFELDER R.R., MICHALÍK J., MÖNNIG E., NOE-NYGAARD N., PÁLFY J., PINT A., RASSER M.W., REISDORF A.G., SCHMID D.U., SCHWEIGERT G., SURLYK F., WETZEL A., WONG T.E., 2008 – Jurassic. *In*: The Geology of Central Europe. Volume 2: Mesozoic and Cenozoic (Ed. T. McCann). The Geological Society of London, Bath. https://doi.org/10.1144/CEV2P.2.

PIEŃKOWSKI G., HODBOD M., ULLMANN C.V., 2016 – Fungal decomposition of terrestrial organic matter accelerated Early Jurassic climate warming. *Scientific Reports*, **6**: 31930. https://doi.org/10.1038/srep31930.

PIEŃKOWSKI G., HESSELBO S.P., BARBACKA M., LENG M.J., 2020 – Non-marine carbon-isotope stratigraphy of the Triassic–Jurassic transition in the Polish Basin and its relationships to organic carbon preservation, pCO_2 and palaeotemperature. *Earth-Science Reviews*, **210**: 103383. https://doi.org/10.1016/j.earscirev.2020.103383.

PIEŃKOWSKI G., UCHMAN A., NINARD K., HESSELBO S.P., 2021 – Ichnology, sedimentology, and orbital cycles in the hemipelagic Early Jurassic Laurasian Seaway (Pliensbachian, Cardigan Bay Basin, UK). *Global and Planetary Change*, **207**: 103648. https://doi.org/10.1016/j.gloplacha.2021.103648.

PIEŃKOWSKI G., UCHMAN A., NINARD K., PAGE K.N., HESSELBO S.P., 2024 – Early Jurassic extrinsic solar system dynamics versus intrinsic Earth processes – Toarcian sedimentation and benthic life in deep-sea contourite drift facies, Cardigan Bay Basin, UK. *Progress in Earth and Planetary Sciences*, **11**: 18. https://doi.org/10.1186/s40645-024-00612-3.

PORTER S.J., SMITH P.L., CARUTHERS A.H., HOU P., GRÖCKE D.R., SELBY D., 2014 – New high resolution geochemistry of Lower Jurassic marine sections in western North America: A global positive carbon isotope excursion in the Sinemurian? *Earth and Planetary Science Letters*, **397**: 19–31. https://doi.org/10.1016/j.epsl.2014.04.023.

POWELL J.H., 2010 – Jurassic sedimentation in the Cleveland Basin: A review. *Proceedings of the Yorkshire Geological Society*, **58**: 21–72. https://doi.org/10.1144/pygs.58.1.278.

RAUP D.M., SEPKOSKI J.J., 1982 – Mass extinctions in the marine fossil tecord. *Science*, **215**: 1501–1503. https://doi.org/10.1126/science.215.4539.1501.

RIDING J.B., LENG M.J., KENDER S., HESSELBO S.P., FEIST-BURKHARDT S., 2013 – Isotopic and palynological evidence for a new Early Jurassic environmental perturbation. *Palaeogeography, Palaeoclimatology, Palaeoecology*, **374**: 16–27. http://dx.doi.org/10.1016/j.palaeo.2012.10.019.

RUEBSAM W., MAYER B., SCHWARK L., 2019 – Cryosphere carbon dynamics control early Toarcian global warming and sea level evolution. *Global and Planetary Change*, **172**: 440–453. https://doi.org/10.1016/j.gloplacha.2018.11.003.

RUEBSAM W., REOLID M., SABATINO N., MASETTI D., SCHWARK L., 2020 – Molecular paleothermometry of the early Toarcian climate perturbation. *Global and Planetary Change*, **195**: 103351, https://doi.org/10.1016/j.gloplacha.2020.103351.

RUHL M., DEENEN M.H.L., ABELS H.A., BONIS N.R., KRIJGSMAN W., KÜRSCHNER W.H., 2010 – Astronomical constraints on the duration of the early Jurassic Hettangian stage and recovery rates following the end-Triassic mass extinction (St. Audrie's Bay/East Quantoxhead, UK). *Earth and Planetary Science Letters*, **296**: 262–276. https://doi.org/10.1016/j.epsl.2010.04.008.

RUHL M., HESSELBO S.P., HINNOV L.A., JENKYNS H.C., XU W., STORM M., RIDING J.B., MINISINI D., ULLMANN C.V., LENG M.J., 2016 – Astronomical constraints on the duration of the Early Jurassic Pliensbachian Stage and global climatic fluctuations. *Earth and Planetary Science Letters*, **455**: 149–165. https://doi.org/10.1016/j.epsl.2016.08.038.

RUHL M., HESSELBO S.P., AL-SUWAIDI A., JENKYNS H.C., DAMBORENEA S.E., MANCEÑIDO M., STORM M., MATHER T., RICCARDI A., 2020 – On the onset of Central Atlantic Magmatic Province (CAMP) volcanism, environmental and carbon-cycle change at the Triassic–Jurassic transition (Neuquén Basin, Argentina). *Earth-Science Reviews*, **208**: 103229. https://doi.org/10.1016/j.earscirev.2020.103229.

RUHL M., HESSELBO S.P., JENKYNS H.C., XU W., SILVA R.L., MATTHEWS K.J., MATHER T.A., MAC NIOCAILL C., RIDING J.B., 2022 – Reduced plate movement controlled onset and timing of Early Jurassic (Toarcian) Karoo-Ferrar large igneous province volcanism and global environmental change. *Science Advances*, **8**: eabo0866. https://doi.org/10.1126/sciadv.abo0866.

SCHALTEGGER U., GUEX J., BARTOLINI A., SCHOENE B., OVTCHAROVA M., 2008 – Precise U-Pb age constraints for end-Triassic mass extinction, its correlation to volcanism and Hettangian post-extinction recovery. *Earth and Planetary Science Letters*, **267**: 266–275. https://doi.org/10.1016/j.epsl.2007.11.031.

SCHOENE B., GUEX J., BARTOLINI A., SCHALTEGGER U., BLACKBURN T.J., 2010 – Correlating the end-Triassic mass extinction and flood basalt volcanism at the100 ka level. *Geology*, **38**: 387–390. https://doi.org/10.1130/G30683.1.

SCHOEPFER S.D., ALGEO T.J., van de SCHOOTBRUGGE B., WHITESIDE J.H., 2022 – The Triassic–Jurassic transition – A review of environmental change at the dawn of modern life. *Earth-Science Reviews*, **232**: 104099. https://doi.org/10.1016/j.earscirev.2022.104099.

SCHÖLLHORN I., ADATTE T., van de SCHOOTBRUGGE B., HOUBEN A., CHARBONNIER G., JANSSEN N., FÖLLMI K.B., 2020 – Climate and environmental response to the break-up of Pangea during the Early Jurassic (Hettangian-Pliensbachian); the Dorset coast (UK) revisited. *Global and Planetary Change*, **185**: 103096. https://doi.org/10.1016/j.gloplacha.2019.103096.

SELLWOOD B.W., 1970 – The relation of trace fossils to small scale sedimentary cycles in the British Lias. *In*: Trace Fossils (Eds. T.R. Crimes, J.C. Harper). *Geological Journal Special Isssue*, **3**: 489–504.

SHA J., OLSEN P.E., PAN Y., XU D., WANG Y., ZHANG X., YAO X., VAJDA V., 2015 – Triassic–Jurassic climate in continental high-latitude Asia was dominated by obliquity-paced variations (Junggar Basin, Ürümqi, China). *Proceedings of the National Academy of Sciences*, **112**: 3624–3629. https://doi.org/10.1073/pnas.150113711.

SMITH D.G., 1989 – Stratigraphic correlation of presumed Milankovitch cycles in the Blue Lias (Hettangian to earliest Sinemurian), England. *Terra Nova*, **1**: 457460. https://doi.org/10.1111/j.1365-3121.1989.tb00410.x.

STORM M.S., HESSELBO S.P., JENKYNS H.C., RUHL M., ULLMANN C.V., XU W., LENG M.J., RIDING J.B., GORBANENKO O., 2020 – Orbital pacing and secular evolution of the Early Jurassic carbon cycle. *Proceedings of the National Academy of Sciences*, **117**: 3974–3982. https://doi.org/10.1073/pnas.1912094117.

STORM M.S., HESSELBO S.P., JENKYNS H.C., RUHL M., AL-SUWAIDI A.H., PERCIVAL L.M.E., MATHER T.A., DAMBORENEA S.E., MANCEÑIDO M.O., RICCARDI A.C., 2024 – Integrated Stratigraphy for Pliensbachian and Toarcian strata from the northern Neuquén Basin, Argentina. *Newsletters on Stratigraphy*, **57**, 4: 389–412. https://doi.org/10.1127/nos/2024/0817.

SUAN G., PITTET B., BOUR I., MATTIOLI E., DUARTE L.V., MAILLIOT S., 2008 – Duration of the Early Toarcian carbon isotope excursion deduced from spectral analysis: Consequence for its possible causes. *Earth and Planetary Science Letters*, **267**: 666–679. https://doi.org/10.1016/j.epsl.2007.12.017.

SUAN G., MATTIOLI E., PITTET B., LÉCUYER C., SUCHÉRAS-MARX B., DUARTE L.V., PHILIPPE M., REGGIANI L., MARTINEAU F., 2010 – Secular environmental precursors to Early Toarcian (Jurassic) extreme climate changes. *Earth and Planetary Science Letters*, **290**: 448–458. https://doi.org/10.1016/j.epsl.2009.12.047.

TAPPIN D.R, CHADWICK R.A, JACKSON A.A., WINGFIELD R.T.R., SMITH N.J.P., 1994 – Geology of Cardigan

Bay and the Bristol Channel, United Kingdom Offshore Regional Report, British Geological Survey, HMSO.

THÖLE H., BORNEMANN A., HEIMHOFER U., LUPPOLD F.W., BLUMENBERG M., DOHRMANN R., ERBACHER J., 2020 – Using high-resolution XRF analyses as a sequence stratigraphic tool in a mudstone-dominated succession (Early Cretaceous, Lower Saxony Basin, Northern Germany). *The Depositional Record*, **6**: 236–258. https://doi.org/10.1002/dep2.83.

ULLMANN C.V., BOYLE B., DUARTE L.V., HESSELBO S.P., KASEMANN S., KLEIN T., LENTON T., PIAZZA V., ABERHAN M., 2020 – Warm afterglow from the Toarcian Oceanic Anoxic Event drives the success of deep-adapted brachiopods. *Scientific Reports*, **10**: 6549. https://doi.org/10.1038/s41598-020-63487-6.

ULLMANN C.V., SZŰCS D., JIANG M., HUDSON A.J.L., HESSELBO S.P., 2021 – Geochemistry of macrofossil, bulk rock, and secondary calcite in the Early Jurassic strata of the Llanbedr (Mochras Farm) drill core, Cardigan Bay Basin, Wales, UK. *Journal of the Geological Society of London*, **179**: jgs2021-018. https://doi.org/10.1144/jgs2021-018.

ULLMANN C.V., DAMASCHKE M., HESSELBO S.P., JIANG M., LAWRENCE K., LENG M.J., MATTIOLIE E., BANCALINE J., PAGE K.N., PUDAL N., RUHL M., SILVA R. 2025 – An integrated biostratigraphy and chemostratigraphy for the dawn of the Jurassic (the Hettangian stage in the Cheshire Basin, UK). *Journal of Earth Science*, https:/doi.org/10.1007/s12583-025-0205-6.

van BUCHEM F.S.P., McCAVE I.N., 1989 – Cyclic sedimentation patterns in Lower Lias mudstones of Yorkshire (GB). *Terra Nova*, **1**: 461–467. https://doi.org/10.1111/j.1365-3121.1989.tb00411.x.

van BUCHEM F.S.P., KNOX R.W.O'B., 1998 – Lower and Middle Jurassic depositional sequences of Yorkshire (UK). *In*: Mesozoic–Cenozoic Sequence Stratigraphy of European Basins (Eds. P.C. de Graciansky *et al.*). *Society for Sedimentary Geology* (SEPM), *Special Publication*, **60**: 545–559.

van BUCHEM F.S.P., MELNYK D.H., McCAVE I.N., 1992 – Chemical cyclicity and correlation of Lower Lias mudstones using gamma ray logs, Yorkshire, UK. *Journal of the Geological Society of London*, **149**: 991–1002. https://doi.org/10.1144/gsjgs.149.6.0991.

van BUCHEM F.S.P., McCAVE I.N., WEEDON G.P., 1994 – Orbitally induced small-scale cyclicity in a siliciclastic epicontinental setting (Lower Lias, Yorkshire, UK). *In*: Orbital Forcing and Cyclic Sequences (Eds. P.L. De Boer, D.G. Smith). *IAS Special Publication*, **19**: 345–366. https://doi.org/10.1002/9781444304039.ch22.

van de SCHOOTBRUGGE B., BACHAN A., SUAN G., RICHOZ S., PAYNE J.L., 2013 – Microbes, mud and methane: Cause and consequence of recurrent Early Jurassic anoxia following the end-Triassic mass extinction. *Palaeontology*, **56**: 685–709. https://doi.org/10.1111/pala.12034.

WALTHAM D., 2015 – Milankovitch period uncertainties and their impact on cyclostratigraphy. *Journal of Sedimentary Research*, **85**: 990–998. https://doi.org/10.2110/jsr.2015.66.

WATERHOUSE H.K., 1999 – Regular terrestrially derived palynofacies cycles in irregular marine sedimentary cycles, Lower Lias, Dorset, UK. *Journal of the Geological Society, London*, **156**: 1113–1124. https://doi.org/10.1144/gsjgs.156.6.1113.

WEEDON G.P., 1986 – Hemipelagic shelf sedimentation and climatic cycles: The basal Jurassic (Blue Lias) of South Britain. *Earth and Planetary Science Letters*, **76**: 321–335. https://doi.org/10.1016/0012-821X(86)90083-X.

WEEDON G.P., JENKYNS H.C., 1999 – Cyclostratigraphy and the Early Jurassic time scale: Data from the Belemnite Marls, Dorset, southern England. *Geological Society of America Bulletin*, **111**: 1823–1840. https://doi.org/10.1130/0016-7606(1999)-111<1823:CATEJT>2.3.CO;2.

WEEDON G.P., JENKYNS H.C., COE A.L., HESSELBO S.P., 1999 – Astronomical calibration of the Jurassic time-scale from cyclostratigraphy in British mudrock formations. *Philosophical Transactions of the Royal Society A: Mathematical, Physical and Engineering Sciences*, **357**: 1787–1813, https://doi.org/10.1098/rsta.1999.0401.

WEEDON G.P., JENKYNS H.C., PAGE K.N., 2018 – Combined sea-level and climate controls on limestone formation, hiatuses and ammonite preservation in the Blue Lias Formation, South Britain (uppermost Triassic–Lower Jurassic). *Geological Magazine*, **155**: 1117–1149. https://doi.org/10.1017/S001675681600128X.

WEEDON G.P., PAGE K.N., JENKYNS H.C., 2019 – Cyclostratigraphy, stratigraphic gaps and the duration of the Hettangian Stage (Jurassic): insights from the Blue Lias Formation of southern Britain. *Geological Magazine*, **156**: 1469–1509. https://doi.org/10.1017/S0016756818000808.

WIGNALL P.B., 2001 – Large igneous provinces and mass extinctions. *Earth-Science Reviews*, **53**: 1–33. https://doi.org/10.1016/S0012-8252(00)00037-4.

WIGNALL P.B., ATKINSON J.W., 2020 – A two-phase end-Triassic mass extinction. *Earth-Science Reviews*, **208**: 103282. https://doi.org/10.1016/j.earscirev.2020.103282.

WOOD A., WOODLAND A., 1968 – Borehole at Mochras, West of Llanbedr, Merionethshire. *Nature*, **219**: 1352–1354. https://doi.org/10.1038/2191352a0.

WOODLAND A. (Ed.), 1971 – The Llanbedr (Mochras Farm) Borehole. *Institute of Geological Sciences, Report*, **71/18**: 1–116.

WOTZLAW J.-F., GUEX J., BARTOLINI A., GALLET Y., KRYSTYN L., MCROBERTS C.A., TAYLOR D., SCHOENE B., SCHALTEGGER U., 2014 – Towards accurate numerical calibration of the Late Triassic: High-precision U-Pb geochronology constraints on the duration of the Rhaetian. *Geology*, **42**: 571–574. https://doi.org/10.1130/G35612.1.

WU Y., MALINVERNO A., MEYERS S.R., HINNOV L.A., 2024 – A 650-Myr history of Earth's axial precession frequency and the evolution of the Earth-Moon system derived from cyclostratigraphy, *Science Advances*, **10/42**. https://doi.org/10.1126/sciadv.ado2412

XU W., RUHL M., HESSELBO S.P., RIDING J.B., JENKYNS H.C., 2017 – Orbital pacing of the Early Jurassic carbon cycle, black-shale formation and seabed methane seepage. *Sedimentology*, **64**: 127–149. https://doi.org/10.1111/sed.1232.

ZIEGLER P.A., 1990 – Geological Atlas of Western and Central Europe. 2nd Edition, Shell Internationale Petroleum Mij. B.V. and Geological Society, London.